Semi–analytical method for the identification of inclusions by air–cored coil interaction in ferromagnetic media

Panayiotis Vafeas, Anastassios Skarlatos, Theodoros Theodoulidis, Dominique Lesselier

Semianalytical method for the identification of inclusions by air-cored coil interaction in ferromagnetic media

Panayiotis Vafeas[1], Anastassios Skarlatos[2], Theodoros Theodoulidis[3], Dominique Lesselier[4]

1Department of Chemical Engineering, University of Patras, 26504 Patras, Greece
2Laboratoire de Simulation et de Modélisation Électromagnétique, CEA-LIST, 91191 Gif-sur-Yvette, France
3Department of Mechanical Engineering,; University of Western Macedonia, 50132 Kozani, Greece
4Laboratoire des Signaux et Systèmes, CNRS-CentraleSupélec, 91192, Gif-sur-Yvette, France

The magnetostatic harmonic fields scattered by a near-surface air inclusion of arbitrary shape, embedded in a conductive ferromagnetic medium and illu-minated by a current-carrying coil, are investigated. The scattering domain is separated into homogeneous subdomains under the assumption of a suitable truncation at a long distance from the incident source, whereas a perfect mag-netic boundary condition is implied. The introduced methodology addresses the full coupling between the two interfaces, ie, the plane that distinguishes the half-space ferromagnetic material from the open air and the arbitrary surface among the inclusion and the ferromagnetic region. Therein, continuity condi-tions are applied in a rigorous way, while the expected behavior of the fields, either as ascending or as descending, are taken into account. The potentials associated with the half-space are expanded via cylindrical harmonic eigen-functions, while those related with the inclusion's arbitrary geometry admit generalized-type formalism. However, since the transmission conditions involve potentials with different eigenexpansions, we are obliged to rewrite cylindri-cal to generalized functions and vice versa, obtaining handy relationships in terms of easy-to-handle integrals, where orthogonality then is feasible. Once done, the calculation of the exact solutions leads to infinite linear algebraic sys-tems, manipulated through standard cut-off techniques. Thus, we obtain the implicated fields in a general analytical and compact fashion, independent of the inclusion's geometry. We demonstrate the efficiency of the analytical model approach, assuming the degenerate case of a spherical inclusion, whereas the air-cored coil simulation via a numerical procedure validates our method. The calculation is very fast, rendering it suitable for use with parametric inversion algorithms.

KEYWORDS

air-cored coil, arbitrary inclusions, harmonic analysis, nondestructive testing

1 - INTRODUCTION

Maxwell's electromagnetic theory for the scattering interaction of arbitrarily shaped targets, embedded within different media and illuminated by a variety of primary sources, operating at several frequencies, has always been in the frontline of the scientific research. Indeed, practical applications range widely, eg, from eddy current testing of conducting materials

to light scattering from particles in optics and orebody detection in geophysics. By deciphering the implicated fields, information about main parameters like orientations, sizes, shapes, magnetic, and electric properties of the anomalies brings insight to the field behavior. However, this is not an easy task, since the inverse problem cannot be tackled in robust fashion unless proper models of the field interaction and efficient mathematical tools are available.

General principles of electromagnetism,[1] combined with scattering theory[2] and the multidisciplinary effect of useful mathematical methods,[3] provide the environment for making available the elementary bricks of an inversion scheme.[4] The motivation of this study comes from interesting applications within the field, indicatively referring to detection of inclusions in two-phase composites,[5,6] Earth's subsurface electromagnetic probing for mineral exploration,[7] identification of cavities,[8] or other underground detections such as unexploded ordnance[9,10] and buried objects,[11] and even scattering by chiral material either in chiral or nonchiral environments.[12-15] Besides, two of the authors have been involved the last decade with several cases related to the retrieval of metallic objects of different shapes and sizes with magnetic dipolar excitation.[16-23]

On the other hand, near surface phenomena are of theoretical interest and practical importance, particularly, in the domain of optics. The first successful attempt of deriving a general solution for the electromagnetic scattering of a planar monochromatic wave by a homogeneous sphere in a homogeneous infinite medium is in the classical paper of Mie.[24] Thereafter, numerous researchers studied the area, like in the work of Bobbert and Vlieger,[25] where the authors constructed an analytical solution for the problem of light scattering by a sphere in a nonabsorbing medium placed on a plane substrate. Almost the same problem was treated in the work of Videen[26] with the difference of assuming that the implicated scattered fields emanating from the sphere, impinge upon the substrate along the normal direction of propagation.

Similar to the optical scattering handling, one could refer to the work of Theodoulidis et al,[27] where the eddy current flow in a conducting sphere induced by an arbitrary current source in the air has been calculated based on the second-order vector potential formulation, while operating at low frequencies still offers encouraging perspective to this direction. The low-frequency electromagnetic scattering problem of a near-surface hollow spherical inclusion is as an example, solved by means of a modal approach.[28] Therein, the authors considered the field negligible at a reasonably long distance from the region of scattering activity and truncated the solution domain using a Dirichlet's boundary condition. This finds application to a number of important induction problems. For instance, we mention the eddy current probe interaction with corner discontinuities,[29] and boreholes, such as the impedance of an induction coil at the opening of a borehole in a conductor[30] and the solution to the eddy current induction problem in a conducting half-space with either a vertical cylindrical borehole[31] or a cylindrical hole parallel to the surface.[32] However, the addition of a second boundary of different geometry, such as the planar surface of a half-space, complicates the problem substantially.

Inductive electromagnetic means within the area of magnetostatics, currently employed in the exploration of defects in ferromagnetic materials, often calls for an intensive use, at the modeling stage and at the inversion stage, of analytically demanding tools of field calculation. Hence, the already ample library of scattering by simple shapes using analytical methods is open to accept new analytical results. This paper describes how to build a versatile set of mathematical tools to infer information about a hollow inclusion of arbitrary shape, position, and orientation, embedded near the surface of a ferromagnetic medium. The primary source is an air-cored coil set above the specimen's plane interface. The direct scattering problem is then composed with respect to the divergence-free magnetostatic fields, written in terms of scalar harmonic potentials.

Based on the truncated region eigenfunction expansion technique,[28] we confine the solution domain by a cylindrical half-space area, where its bottom and the surrounding surface is considered to be far away from the inclusion, and the interface between the ferromagnetic material and the open air, so as the magnetostatic field be negligible therein. For modeling purposes, the domain of interest is separated into homogeneous subdomains, whereas standard continuity conditions yield the coupling between the two interfaces. Perfect magnetic conditions secure the vanishing of the magnetic field on the cylindrical walls, while the behavior of the involved potentials as we move either upwards or downwards is inherited to the corresponding forms of the expansions. The scattering problem is solved by means of a modal approach, where the potentials associated with the half-space are expanded into cylindrical harmonic eigenfunctions,[33,34] while those related with the inclusion's arbitrary geometry imply general eigenexpansions, depending on the type of the fitted coordinate system of each case. Although, this alternative behavior is conveyed to the transmission conditions and their ostensibly trivial manipulation becomes impossible unless we apply conversion relations between cylindrical and generalized eigenfunctions. The key point is the exploitation of the common translational axis between any orthogonal clockwise coordinate system (eg, spherical, spheroidal, or ellipsoidal are the common cases) and the cylindrical one used for the treatment of the planar and the arbitrary interface, respectively. However, this method results into expressions

that include integrals, which must be evaluated, either numerically or through hybrid elaboration or even in a pure analytical fashion, once a particular geometry for the inclusion is assumed. When done, the conditions are handled via the enforcement of proper orthogonality rules to obtain infinite linear algebraic systems, solved via well-known cut-off techniques. The presented approach is rigorous, in the sense that no approximation is made apart from the vanishing fields at far distances. Consequently, we obtain the potential fields, hence the corresponding magnetostatic vectors, in terms of closed-form solutions, independently of the air inclusion's shape. Such a general confrontation is extremely useful, since the shape of cracks is arbitrary in most cases; thus, the corresponding modeling requires the proper coordinate system that fits the geometry of the inclusion.

The analytical part of this paper is supplemented with the application of our implicit technique to the case of a complete isotropic inclusion under the aim to reproduce the spherical case as an example of the generalized results. The corresponding integrals are calculated in an analytical-like manner with the aid of complicated formulae[35,36] that interconnects cylindrical and spherical eigenfunctions,[33,34] while the final expressions are validated via a numerical procedure of air-cored coil simulation. Nevertheless, the difficulty from the spherical to the spheroidal system and then to the much complicated ellipsoidal one, which represents the complete anisotropy of the three-dimensional (3-D) space, is increasing due to the more elaborating harmonic eigenfunctions related to each applied geometry; therefore, the introduction of the general methodology is imperative.

The rest of this contribution is organized as follows. In Section 2, a detailed physical development and the theoretical basis via an analytical mathematical formulation is sketched. The problem itself is set in terms of the cylindrical configuration of the surrounding domain, incorporating the general attributes of an inclusion of arbitrary shape, orientation, and location. Then, the generalized solution technique at hand is explained step-by-step in Section 3, where the magnetostatic fields are provided through compact closed-form formulae of the corresponding harmonic potentials. Section 4 is devoted to an example of a spherical-type air inclusion, whereas the relative analysis is recovered by the introduced methodology and some interesting special cases are discussed, while further manipulation of the spherical modes for field illustration is also available. The main article closes with Section 5, which contains a validation of the depicted results with a numerical simulation. Finally, a brief conclusion containing an outline of our work and future steps follows in Section 6, while an updated reference list is presented immediately after.

2 - PHYSICAL AND MATHEMATICAL DEVELOPMENT

The configuration of the problem is sketched in Figure 1. A general arbitrarily shaped void inclusion of air permeability μ_0 is embedded in an otherwise ferromagnetic half-space with permeability $\mu > \mu_0$, obtaining the relative permeability as

$$\mu_r = \frac{\mu}{\mu_0} > 1. \tag{1}$$

We mention that only the linear case is considered in this study, while we assume that the inclusion is entirely contained in the half-space. A static magnetic field is exerted upon the medium under consideration either by means of a current coil or a permanent magnet. These are the two of the most common ways for magnetizing the specimen in magnetic flux

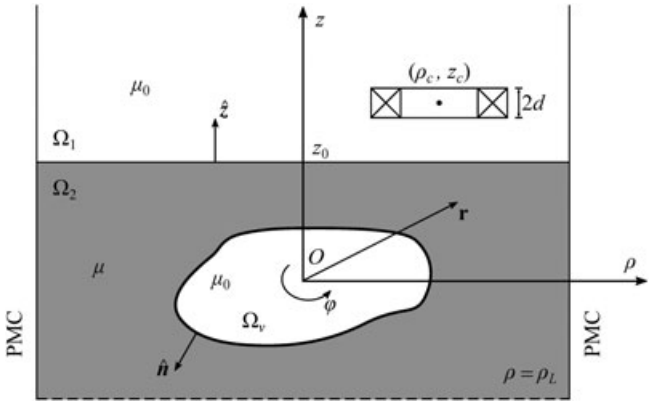

FIGURE 1 Arbitrarily shaped air inclusion embedded within a conducting half-space, illuminated by a cylindrical coil. Lateral view with the cylindrical coordinate system of the truncated domain, using a perfect magnetic conductor (PMC) condition

leakage and magnetic particle nondestructive applications. Among the two frequently used methods, we only consider the excitation technique via the current coil.

Our application is involved with smooth and 3-D environments $\Omega\left(\mathbb{R}^3\right) \equiv \Omega$, which could be either bounded with surrounding boundary surface $\partial\Omega\left(\mathbb{R}^3\right) \equiv S$ or unbounded, taking as $S \to +\infty$, when the case might be. For the treatment of the reflection terms emerging from the interaction with the inclusion, and the field inside the air void, it is much more convenient to work with the local coordinate system conformal with the geometry of the inclusion's surface. Henceforth, since the proceeding method is independent of the 3-D geometry of the inclusion, then every field related to it can be written in terms of the spatial position vector $\mathbf{r} = x_1\hat{\boldsymbol{x}}_1 + x_2\hat{\boldsymbol{x}}_2 + x_3\hat{\boldsymbol{x}}_3$, expressed via the Cartesian basis $\hat{\boldsymbol{x}}_j$ for $j = 1, 2, 3$ in Cartesian coordinates (x_1, x_2, x_3), where this dependence is sometimes omitted for writing convenience. On the other hand, to proceed to the development of the solution, we fix a global reference frame, whose origin coincides with the center of symmetry of the inclusion. Given the rotational symmetry of the configuration, it is meaningful enough to work in circular cylindrical coordinates (ρ, φ, z) as far as the global reference frame is concerned and the fields associated with that. This dependence will be designated for any involved function via

$$\mathbf{r} \equiv \sum_{i=1}^{3} x_i\hat{\boldsymbol{x}}_i = z\hat{\boldsymbol{x}}_1 + \rho\cos\varphi\hat{\boldsymbol{x}}_2 + \rho\sin\varphi\hat{\boldsymbol{x}}_3 \text{ for } \rho \in [0, +\infty)\,, \varphi \in [0, 2\pi) \text{ and } z \in (-\infty, +\infty)\,, \tag{2}$$

where the z-axis of symmetry is normal to the half-space interface and the other two axes are located properly so as to obtain the dextral system (2).

For modeling purposes and since we deal with a magnetostatic problem, we separate the domain of interest into homogeneous subdomains, whereas the solution can be derived in a truncated region along the direction of ρ at a distance equal to ρ_L. For simplicity, we consider a perfect magnetic boundary condition at truncation limit $\rho = \rho_L$, the choice of this condition being arbitrary, since the field is negligible there. We also assume that the distance of the half-space free surface from the origin is equal to z_0, while the bottom boundary of our system is located at $z = -z_b$. The aforementioned restrictions confine the cylindrical area of field activity Ω to $\rho \in [0, \rho_L)$, $\varphi \in [0, 2\pi)$, and $z \in (-z_b, +\infty)$. However, here, we are obliged to remark that as for now we deal with the case of a ferromagnetic half-space, which means that the bottom is considered to be far away from both the inclusion and the interface, ie, $z_b \gg 0$ and $z_b \gg z_0$, respectively, leading to $-z_b \to -\infty$, an assumption that coincides with physical reality. On the other hand, the known source is comprised by a current coil of inner and outer radius, r_{in} and r_{out}, respectively, and thickness $2d$, which is set at (ρ_c, φ, z_c) for every $\varphi \in [0, 2\pi)$. To this end, since we are merely interested in the solution just above the half-space interface, we restrict our analysis to the source-free region between the coil and the interface, ie, $z < z_c - d$. In the same manner, the lower infinite limit of the z-variable is not of physical, hence mathematical, interest; therefore, we need to know the field distribution just above the void inclusion for $z > 0$. Recapitulating, the domain of field activity Ω yields $\rho \in [0, \rho_L)$, $\varphi \in [0, 2\pi)$ and $z \in (0, z_c - d)$, where the restrictions to the intervals have been made without loss of generality, while this area, for the purposes of the analysis, is furtherly distinguished to different regions. In details, the air half-space will be referred to as region

$$\Omega_1 = \left\{(\rho, \varphi, z)\,, \in \mathbb{R}^3 \,:\, \rho \in [0, \rho_L), \varphi \in [0, 2\pi), z \in (z_0, z_c - d)\right\} \subset \Omega, \tag{3}$$

while the ferromagnetic half-space will be addressed as

$$\Omega_2 = \left\{(\rho, \varphi, z)\,, \in \mathbb{R}^3 \,:\, \rho \in [0, \rho_L), \varphi \in [0, 2\pi), z \in (0, z_0)\right\} - \Omega_v \subset \Omega, \tag{4}$$

whereas their common boundary is defined as $\partial\Omega_{1,2} \equiv S_{1,2}$ with outward unit normal vector $\hat{\boldsymbol{n}}_{1,2} \equiv \hat{\boldsymbol{z}}$, $\hat{\boldsymbol{z}}$ being the coordinate vector in the direction of the axis of symmetry of the cylindrical system. The bounded domain Ω_v stands for the arbitrary void with a closed surrounding surface $\partial\Omega_v \equiv S_v$, which is specified by the outward unit normal vector $\hat{\boldsymbol{n}}_v \equiv \hat{\boldsymbol{n}}$. Let us presume that, with respect to the origin of the implied coordinate system, the air volume Ω_v occupies a space of a surface characteristic variable R_v, as conveniently referred, which is introduced as a helpful geometric parameter to our generalized mathematical technique, and it is actually the so-called "radial" featured component, running on S_v, ie, $R_v \equiv R_v(S_v)$. As a matter of fact, the nature of this domain and its surface characteristic variable depends upon the particular geometry of the inclusion. Note that a simply connected 3-D inclusion can be adequately approximated by sphere, in the simplest case, by either a prolate or oblate spheroid, increasing the complexity and by an ellipsoid with three different axes, tilted with respect to the normal to the half-space interface. The latter is considered to be general, incorporating both physical and mathematical tools. Nevertheless, since the spherical geometry occurs frequently within solutions of such-like problems, it is interesting to treat also this problem in the framework of the current analysis, to use it as a limiting case for controlling the solution of the spheroidal and the ellipsoidal inclusion. However, our main purpose is to provide

general formulae for any geometrical shape matching the inclusion and demonstrate the theoretical technique with an application, where the inclusion is considered to retain spherical structure.

The magnetostatic vector fields can be expressed in the source-free regions in terms of the corresponding magnetic scalar potentials via

$$\mathbf{B}_k(\mathbf{r}) = -\nabla\Phi_k(\mathbf{r}) \text{ with } \nabla\cdot\mathbf{B}_k(\mathbf{r}) = 0 \Rightarrow \Delta\Phi_k(\mathbf{r}) = 0 \text{ for } \mathbf{r}\in\Omega \text{ and } k = s, a, f, c, v, \tag{5}$$

identifying the potentials as functions that satisfy Laplace's equation. Specifically, in region Ω_1, the fields can be decomposed into two terms, one for the known source contribution Φ_s and one from the reflection from the interface to the air Φ_a, providing in view of the constitutive equations (5)

$$\Phi_1(\mathbf{r}) = \Phi_s(\mathbf{r}) + \Phi_a(\mathbf{r}) \text{ or } \mathbf{B}_1(\mathbf{r}) = \mathbf{B}_s(\mathbf{r}) + \mathbf{B}_a(\mathbf{r}) \text{ for } \mathbf{r}\in\Omega_1, \tag{6}$$

while region Ω_2 involves two boundaries, the one of the half-space and the inclusion's boundary. Hence, two terms are needed, each one being associated with each boundary. Letting Φ_f signify the transmitted term associated with the half-space interface and Φ_c be the reflection from the inclusion, the total fields, given within (5), can be decomposed as

$$\Phi_2(\mathbf{r}) = \Phi_f(\mathbf{r}) + \Phi_c(\mathbf{r}) \text{ or } \mathbf{B}_2(\mathbf{r}) = \mathbf{B}_c(\mathbf{r}) + \mathbf{B}_f(\mathbf{r}) \text{ for } \mathbf{r}\in\Omega_2. \tag{7}$$

Finally, we denote Φ_v the potential inside the inclusion Ω_v, which generates the corresponding magnetic field $\mathbf{B}_v = -\nabla\Phi_v$. Once the harmonic potentials Φ_k are calculated, then the magnetostatic fields $\mathbf{B}_k$ are evaluated through (5) for any $k = s, a, f, c, v$, where the gradient and the Laplacian differential operators are being interrelated with the potential fields in both their invariant and cylindrical form, ie,

$$\nabla \equiv \sum_{i=1}^{3}\hat{\boldsymbol{x}}_i\frac{\partial}{\partial x_i} = \hat{\boldsymbol{\rho}}\frac{\partial}{\partial\rho} + \frac{\hat{\boldsymbol{\varphi}}}{\rho}\frac{\partial}{\partial\varphi} + \hat{\boldsymbol{z}}\frac{\partial}{\partial z} \text{ and } \Delta \equiv \sum_{i=1}^{3}\frac{\partial^2}{\partial x_i^2} = \frac{1}{\rho}\frac{\partial}{\partial\rho}\left(\rho\frac{\partial}{\partial\rho}\right) + \frac{1}{\rho^2}\frac{\partial^2}{\partial\varphi^2} + \frac{\partial^2}{\partial z^2} \tag{8}$$

for every $\rho\in[0,\rho_L)$, $\varphi\in[0,2\pi)$ and $z\in(0,z_c-d)$. Definitions (8) yield expressions via the Cartesian basis $\hat{\boldsymbol{x}}_j$ for $j = 1, 2, 3$ and in terms of the coordinate vectors of the circular cylindrical coordinate system, those being

$$\hat{\boldsymbol{\rho}} = -\frac{\partial\hat{\boldsymbol{\varphi}}}{\partial\varphi} = \cos\varphi\hat{\boldsymbol{x}}_2 + \sin\varphi\hat{\boldsymbol{x}}_3, \hat{\boldsymbol{\varphi}} = \frac{\partial\hat{\boldsymbol{\rho}}}{\partial\varphi} = -\sin\varphi\hat{\boldsymbol{x}}_2 + \cos\varphi\hat{\boldsymbol{x}}_3 \text{ and } \hat{\boldsymbol{z}} = \hat{\boldsymbol{x}}_1, \tag{9}$$

completing our analysis with regard to the magnetostatic and potential fields.

The aforementioned partial differential equations are supplemented by the appropriate boundary, continuity and limiting conditions. The only boundary conditions refer to the imposition of the perfectly magnetic conductor property at the truncation surface $\rho = \rho_L$ and regularity of the fields on the axis of symmetry of the specimen for $\rho = 0$, which imply

$$\mathbf{B}_k(\rho_L,\varphi,z) = \mathbf{0} \text{ for every } \varphi\in[0,2\pi) \text{ and } z\in(0,z_c-d) \text{ with } k = s, a, f \tag{10}$$

and

$$\mathbf{B}_k(0,\varphi,z) = \boldsymbol{f}_k(\varphi,z) \text{ for every } \varphi\in[0,2\pi) \text{ and } z\in(0,z_c-d) \text{ with } k = s, a, f, \tag{11}$$

respectively, for the fields associated with the planar interface, $\boldsymbol{f}_k$ for $k = s, a, f$ being vector continuous and regular known functions. On the other hand, the limiting conditions involve all the fields in the sense that, with respect to the air void, Φ_c must be regular at infinity as an exterior field, when Φ_v owes to be bounded at the origin as an interior field, ie,

$$\lim_{|\mathbf{r}|\to+\infty}\Phi_c(\mathbf{r}) = 0 \text{ for } \mathbf{r}\in\Omega_2 \text{ and } \lim_{|\mathbf{r}|\to 0}\Phi_v(\mathbf{r}) = 0 \text{ for } \mathbf{r}\in\Omega_v, \tag{12}$$

respectively, while the behavior of the potentials Φ_s, Φ_a, and Φ_f, as we move upwards (in the case when hypothetically $z_c - d\to+\infty$) or downwards (wishing the lower limit at $z = 0$ to extend at infinity as $z\to-\infty$) along the z-axis, admits

$$\lim_{z\to-\infty}\Phi_s(\mathbf{r}) = 0 \text{ and } \lim_{z\to+\infty}\Phi_a(\mathbf{r}) = 0 \text{ for } \mathbf{r}\in\Omega_1, \text{while } \lim_{z\to-\infty}\Phi_f(\mathbf{r}) = 0 \text{ for } \mathbf{r}\in\Omega_2. \tag{13}$$

Conditions (12) and (13) are supplemented by the continuity restrictions for the total fields on every separable surface, ie, $S_{1,2}$, going with $\hat{\boldsymbol{n}}_{1,2}\equiv\hat{\boldsymbol{z}}$ and S_v, accompanied by $\hat{\boldsymbol{n}}$. Therein, on the interface boundary, continuity of the tangential components of magnetic fields imply

$$\hat{\boldsymbol{z}}\times\mathbf{H}_1(\mathbf{r}) = \hat{\boldsymbol{z}}\times\mathbf{H}_2(\mathbf{r}), \text{where } \mathbf{H}_1(\mathbf{r}) = \frac{1}{\mu_0}\mathbf{B}_1(\mathbf{r}) \text{ and } \mathbf{H}_2(\mathbf{r}) = \frac{1}{\mu}\mathbf{B}_2(\mathbf{r}) \text{ for } \mathbf{r}\in S_{1,2}, \tag{14}$$

while continuity of the normal component of the magnetostatic field provides

$$\hat{\boldsymbol{z}} \cdot \mathbf{B}_1(\mathbf{r}) = \hat{\boldsymbol{z}} \cdot \mathbf{B}_2(\mathbf{r}) \text{ for } \mathbf{r} \in S_{1,2}. \tag{15}$$

Proceeding to the other arbitrary interface between the air cavity and the ferromagnetic medium, we similarly obtain

$$\hat{\boldsymbol{n}} \times \mathbf{H}_2(\mathbf{r}) = \hat{\boldsymbol{n}} \times \mathbf{H}_v(\mathbf{r}), \text{where } \mathbf{H}_2(\mathbf{r}) = \frac{1}{\mu}\mathbf{B}_2(\mathbf{r}) \text{ and } \mathbf{H}_v(\mathbf{r}) = \frac{1}{\mu_0}\mathbf{B}_v(\mathbf{r}) \text{ for } \mathbf{r} \in S_v, \tag{16}$$

concerning the tangential components of the magnetic fields, while

$$\hat{\boldsymbol{n}} \cdot \mathbf{B}_2(\mathbf{r}) = \hat{\boldsymbol{n}} \cdot \mathbf{B}_v(\mathbf{r}) \text{ for } \mathbf{r} \in S_v, \tag{17}$$

in regard to the normal component of the magnetostatic fields.

In summary, we completed the physical and mathematical definition of a well-posed boundary value problem with respect to the identification of arbitrarily shaped inclusions embedded within ferromagnetic material. The problem will be solved for the magnetostatic fields, which satisfy (5) with (6) and (7), accompanied by the appropriately chosen boundary (10) and (11), limiting (12) and (13) and continuity (14) to (17) conditions.

3 - ANALYTICAL FIELD CALCULATION

We develop now the solution for the potentials Φ_k for $k = s, a, f, c, v$ in basis of eigensolutions of the Laplace's equation, since they satisfy (5). Therefore, for the terms associated with the planar interface, we expand them in terms of cylindrical eigenfunctions as

$$\Phi_s(\mathbf{r}) = \sum_{n=-\infty}^{+\infty} e^{\mathrm{i}n\varphi} \sum_{m=1}^{+\infty} C_{n/m}^{(s)} J_n\left(r_n^m \frac{\rho}{\rho_L}\right) e^{r_n^m \frac{z-z_0}{\rho_L}} \text{ for } \mathbf{r} \in \Omega_1, \tag{18}$$

which is the known source field of the current coil, meaning that $C_{n/m}^{(s)}$ for $n \in \mathbb{N}$ and $m \in \mathbb{N}_+^*$ defines a set of imposed well-known constants, while

$$\Phi_a(\mathbf{r}) = \sum_{n=-\infty}^{+\infty} e^{\mathrm{i}n\varphi} \sum_{m=1}^{+\infty} C_{n/m}^{(a)} J_n\left(r_n^m \frac{\rho}{\rho_L}\right) e^{-r_n^m \frac{z-z_0}{\rho_L}} \text{ for } \mathbf{r} \in \Omega_1 \tag{19}$$

and

$$\Phi_f(\mathbf{r}) = \sum_{n=-\infty}^{+\infty} e^{\mathrm{i}n\varphi} \sum_{m=1}^{+\infty} C_{n/m}^{(f)} J_n\left(r_n^m \frac{\rho}{\rho_L}\right) e^{r_n^m \frac{z-z_0}{\rho_L}} \text{ for } \mathbf{r} \in \Omega_2, \tag{20}$$

defining as $\mathbf{r} = (\rho, \varphi, z)$, whereas $C_{n/m}^{(a)}$ and $C_{n/m}^{(f)}$ for $n \in \mathbb{N}$ and $m \in \mathbb{N}_+^*$ are the first set of unknown constant coefficients. The harmonic potential fields (18) to (20) are written in terms of the Bessel functions of the first kind J_n of order $n \in \mathbb{N}$, which are orthogonal as

$$\int_0^{\rho_L} J_n\left(r_n^m \frac{\rho}{\rho_L}\right) J_n\left(r_n^{\overline{m}} \frac{\rho}{\rho_L}\right) \rho \mathrm{d}\rho = \delta_{m\overline{m}} \frac{\rho_L^2}{2} \left[J_{n+1}\left(r_n^m\right)\right]^2 \text{ for } n \in \mathbb{N} \text{ and } m, \overline{m} \geq 1, \tag{21}$$

in view of the delta function $\delta_{m\overline{m}}$ with $m, \overline{m} \geq 1$ and bearing in mind that $J_{-n} = (-1)^n J_n$ for every $n \in \mathbb{N}$. Moreover, their argument is chosen appropriately to automatically satisfy relation (10) with the aid of definitions (5), since we introduce the parameter $r_n^m \in \mathbb{R}$ as the m-root ($m \geq 1$) of order $n \in \mathbb{N}$ of the Bessel functions of the first kind, ie, $J_n\left(r_n^m\right) = 0$. In addition, this situation of an internal problem, as far as potentials (18) to (20) is concerned and by virtue of (11), requires the use of the Bessel functions J_n for $n \geq 0$, which are regular solutions on the axis of symmetry of the circular cylinder; hence, the second set of the Neumann special functions must be excluded, since they become infinite when $\rho = 0$. Specifically, on the z-axis of symmetry, potentials (18) to (20) vanish, except for the case for $n = 0$, whereas $J_0(0) = 1$ and

$$\boldsymbol{f}_k(\varphi, z) = -\nabla\Phi_k(0, \varphi, z) = \sum_{m=1}^{+\infty} C_{0/m}^{(f)} e^{\mathrm{sgn}(k) r_0^m \frac{z-z_0}{\rho_L}} \text{ for every } \varphi \in [0, 2\pi) \text{ and } z \in (0, z_c - d), \tag{22}$$

where $\mathrm{sgn}(k) = +1$ if $k = s, f$ and $\mathrm{sgn}(k) = -1$ if $k = a$. In addition, concerning the z-variable of the aforementioned potentials, the sign of each exponential varies for each case whether they are directed upwards or downwards, meaning that the positive exponent is used for the source field ($k = s$) and the downwards evanescent solution ($k = f$), while the negative one is for the reflection from the interface ($k = a$), so as conditions (13) are immediately fulfilled. Of course, by

setting the argument of the z-variable as $z - z_0$, we simplify our calculations on the planar interface boundary for $z = z_0$, as it will be seen later. Finally, for reasons of clarity, we mention that the φ-dependence of the eigenfunctions involved within (18) to (20), include exponentials with complex variables, which satisfy the orthogonality relationship

$$\int_0^{2\pi} e^{\mathrm{i}n\varphi} e^{-\mathrm{i}\overline{n}\varphi} \mathrm{d}\varphi = 2\pi\delta_{n\overline{n}} = \begin{cases} 2\pi, & n = \overline{n} \\ 0, & n \neq \overline{n} \end{cases} \quad \text{for every } n, \overline{n} \in \mathbb{N}, \tag{23}$$

where $e^{\pm \mathrm{i}n\varphi} = \cos n\varphi \pm i \sin n\varphi$ for any $\varphi \in [0, 2\pi)$ with $n \in \mathbb{N}$ and in terms of the imaginary unit $i = \sqrt{-1}$.

The remaining harmonic potentials Φ_c and Φ_v are associated with the inclusion, and since the primary goal of this article is to choose a convenient notation to keep the analysis in the most compact and general form, the aforementioned fields may assume internal and external general expansions, according to regularity argumentation described earlier, giving

$$\Phi_c(\mathbf{r}) = \sum_{n'} \sum_{m'} C^{(c)}_{n'/m'} U^{(\mathrm{ex})}_{n'/m'}(\mathbf{r}) \text{ with } \Delta U^{(\mathrm{ex})}_{n'/m'}(\mathbf{r}) = 0 \text{ for } \mathbf{r} \in \Omega_2 \text{ with} \forall \left(n', m'\right) \tag{24}$$

and

$$\Phi_v(\mathbf{r}) = \sum_{n'} \sum_{m'} C^{(v)}_{n'/m'} U^{(\mathrm{in})}_{n'/m'}(\mathbf{r}) \text{ with } \Delta U^{(\mathrm{in})}_{n'/m'}(\mathbf{r}) = 0 \text{ for } \mathbf{r} \in \Omega_v \text{ with} \forall \left(n', m'\right). \tag{25}$$

The generalized formalism (24) and (25) is in accordance with the basic harmonic analysis, introduced for the main geometries that could describe an inclusion, ie, for the spherical, the spheroidal, or the ellipsoidal case, where separation of variables in the Laplace's equation admits eigenexpansions of the form (24) and (25). However, each case provides different intervals for the summation indexes n' and m'; hence, we have chosen the symbolism "$\sum_{n'} \sum_{m'} \cdots$" and "$\forall\left(n', m'\right)$" to declare this kind of arbitrariness to our work. On the other hand, the harmonic functions $U^{(\mathrm{in})}_{n'/m'}$ and $U^{(\mathrm{ex})}_{n'/m'}$ for $\forall\left(n', m'\right)$ represent any interior and exterior solution of the Laplace's equation, respectively, written independently of the applied geometry. Under the aim to keep consistency with our generalized technique, we recall the definition of the surface characteristic variable R_v, following any point on S_v and we separate the so-called "radial" part, either interior $G^{(\mathrm{in})}_{n'/m'}(R)$ or exterior $G^{(\mathrm{ex})}_{n'/m'}(R)$, from the "angular" part $g_{n'/m'}(\hat{\mathbf{r}})$ for $\forall\left(n', m'\right)$ of the implicated harmonic eigenfunctions via

$$U^{(\mathrm{in})}_{n'/m'}(\mathbf{r}) = G^{(\mathrm{in})}_{n'/m'}(R)\, g_{n'/m'}(\hat{\mathbf{r}}) \text{ for } \mathbf{r} \in \Omega_v \text{ with } \forall \left(n', m'\right) \tag{26}$$

and

$$U^{(\mathrm{ex})}_{n'/m'}(\mathbf{r}) = G^{(\mathrm{ex})}_{n'/m'}(R)\, g_{n'/m'}(\hat{\mathbf{r}}) \text{ for } \mathbf{r} \in \Omega_2 \text{ with } \forall \left(n', m'\right), \tag{27}$$

denoting as $\mathbf{r} = (R, \hat{\mathbf{r}})$, where the spatial characteristic variable R, as representatively referred, extends from zero to R_v (pointing inside the inclusion) and thereafter from R_v to R_L (pointing outside the inclusion), R_L being the characteristic variable that corresponds to the cylindrical specimen's opening for $\rho = \rho_L$, while $\hat{\mathbf{r}}$ includes the other two variables. Certainly, when $R = R_v$, we move along any point on the interface S_v between the inclusion and the ferromagnetic medium, which is identified by the external unit normal vector $\hat{\boldsymbol{n}} \equiv \hat{\boldsymbol{R}}$, as we now designate it. Since the functions $g_{n'/m'}$ for $\forall\left(n', m'\right)$ comprise the analogous of the surface harmonics in any coordinate system, then we can assume that, for the systems of our interest, they are orthogonal with respect to the general integral

$$\iint_{S_v} h(\hat{\mathbf{r}})\, g_{n'/m'}(\hat{\mathbf{r}})\, \overline{g}_{\overline{n}'/\overline{m}'}(\hat{\mathbf{r}})\, \mathrm{d}S(\hat{\mathbf{r}}) = \mathrm{d}_{n'/m'} \delta_{n'\overline{n}'} \delta_{m'\overline{m}'} \text{ for } \forall \left(n', m'\right) \text{ and } \forall \left(\overline{n}', \overline{m}'\right), \tag{28}$$

where h is a classic weighting function of each system, $d_{n'/m'}$ are the corresponding orthonormalization constants, $\overline{g}_{\overline{n}'/\overline{m}'}$ is the orthogonal form of $g_{n'/m'}$ in (28), and $\delta_{n'\overline{n}'}$ and $\delta_{m\overline{m}'}$ for $\forall \left(n', m'\right)$ and $\forall \left(\overline{n}', \overline{m}'\right)$ stand for typical Kronecker's deltas. Herein, we are also obliged to introduce the differential operators in terms of the generalized variables R and $\hat{\mathbf{r}}$ through a symbolic form as well to match the main orthogonal dextral coordinate systems, that is configured by

$$\nabla' \equiv \sum_{i=1}^{3} \hat{\boldsymbol{x}}_i \frac{\partial}{\partial x_i} = Q(R; \hat{\mathbf{r}})\, \hat{\boldsymbol{R}} \frac{\partial}{\partial R} + \boldsymbol{D}(\hat{\mathbf{r}}; R) \text{ and } \Delta' \equiv \sum_{i=1}^{3} \frac{\partial^2}{\partial x_i^2} = \nabla' \cdot \nabla', \tag{29}$$

where $Q(R; \hat{\mathbf{r}})\, \hat{\boldsymbol{R}} \frac{\partial}{\partial R}$ and $\boldsymbol{D}(\hat{\mathbf{r}}; R)$ coincides with the "radial" and the "angular" part of the gradient operator, respectively. Furthermore, the behavior of the potentials Φ_c from (24) and Φ_v from (25) impose the exterior and the interior character, respectively, so as the remaining limiting condition (12) to be readily satisfied. Concluding, the second set of the unknown constant coefficients $C^{(c)}_{n'/m'}$ and $C^{(v)}_{n'/m'}$ for $\forall \left(n', m'\right)$ that appear within (24) and (25) are to be evaluated accordingly.

We proceed now to the calculation of the undetermined constant coefficients $C^{(a)}_{n/m}$ and $C^{(f)}_{n/m}$ for $n \in \mathbb{N}$ and $m \in \mathbb{N}^*_+$, and $C^{(c)}_{n'/m'}$ and $C^{(v)}_{n'/m'}$ for $\forall\left(n', m'\right)$, provided the constants $C^{(s)}_{n/m}$ for $n \in \mathbb{N}$ and $m \in \mathbb{N}^*_+$ of the excitation field. In order to accomplish that, we have to use the remaining conditions (14) to (17), which by virtue of (1), (6), and (7), imply

$$\hat{\boldsymbol{z}} \times \nabla \left\{ \mu_r \left[\Phi_s \left(\rho, \varphi, z_0 \right) + \Phi_a \left(\rho, \varphi, z_0 \right) \right] - \Phi_f \left(\rho, \varphi, z_0 \right) \right\} = \hat{\boldsymbol{z}} \times \nabla \Phi_c \left(R, \hat{\mathbf{r}} \right) \big|_{z = z_0} \tag{30}$$

and

$$\hat{\boldsymbol{z}} \cdot \nabla \left[\Phi_s \left(\rho, \varphi, z_0 \right) + \Phi_a \left(\rho, \varphi, z_0 \right) - \Phi_f \left(\rho, \varphi, z_0 \right) \right] = \hat{\boldsymbol{z}} \cdot \nabla \Phi_c \left(R, \hat{\mathbf{r}} \right) \big|_{z = z_0} \tag{31}$$

for every $\rho \in [0, \rho_L)$ and $\varphi \in [0, 2\pi)$ on the interface between the open air and the ferromagnetic material, the gradient provided by the cylindrical analogous in relation (8); while taking into account that $\hat{\boldsymbol{n}} \equiv \hat{\boldsymbol{R}}$, we obtain

$$\hat{\boldsymbol{R}} \times \nabla' \Phi_f \left(\rho, \varphi, z \right) \Big|_{R = R_v} = \hat{\boldsymbol{R}} \times \nabla' \left[-\Phi_c \left(R_v, \hat{\mathbf{r}} \right) + \mu_r \Phi_v \left(R_v, \hat{\mathbf{r}} \right) \right] \tag{32}$$

and

$$\hat{\boldsymbol{R}} \cdot \nabla' \Phi_f \left(\rho, \varphi, z \right) \Big|_{R = R_v} = \hat{\boldsymbol{R}} \cdot \nabla' \left[-\Phi_c \left(R_v, \hat{\mathbf{r}} \right) + \Phi_v \left(R_v, \hat{\mathbf{r}} \right) \right] \tag{33}$$

for every $\hat{\mathbf{r}} \in S_v$ on the arbitrary interface between the air cavity and the ferromagnetic medium, the gradient provided now by the invariant formula (29). Even though the continuity equations (30) to (33) seem to be trivial to provide a result, the crucial problem that appears in all of them is that, within each one of these relationships, there always exist potentials with expansions via different kind of eigenfunctions; consequently, the application of orthogonality properties to obtain the constant coefficients is impossible at this stage. Indeed, observing the first double set of conditions (30) and (31), which are written in cylindrical coordinates, it is obvious that, while the potentials on the left-hand side of them admit cylindrical eigenexpansions, the potential on the right-hand side Φ_c is constructed for a general system of coordinates with the gradient ∇ from (8), acting on it. Similarly, the second double set of conditions (32) and (33), which refer to any kind of arbitrary geometry, it is again obvious that, while the potentials on the right-hand side of them are expanded in a generalized coordinate system, the potential Φ_f on the left-hand side assume cylindrical eigenexpansion with the gradient ∇' from (29), acting on it. Consequently, the continuity relationships become useless in their current form, and this makes mandatory the elaboration of the aforementioned conditions to recover much more handy expressions for them. To do so, we are obliged to expand cylindrical eigenexpansions to general eigensolutions and vice versa, where orthogonality then would be feasible. Initially, examining the cylindrical-type conditions (30) and (31), we notice that potential Φ_c, given in (24), contains only the general exterior harmonics $U^{(\mathrm{ex})}_{n'/m'}$ for $\forall\left(n', m'\right)$ from (27), concluding to the fact that only these solutions are needed to be expanded to the corresponding interior cylindrical basis. In that sense,

$$U^{(\mathrm{ex})}_{n'/m'} \left(\mathbf{r} \right) \equiv G^{(\mathrm{ex})}_{n'/m'} \left(R \right) \mathrm{g}_{n'/m'} \left(\hat{\mathbf{r}} \right) = \sum_{n=-\infty}^{+\infty} e^{\mathrm{i}n\varphi} \sum_{m=1}^{+\infty} A^{n'/m'}_{n/m} J_n \left(r^m_n \frac{\rho}{\rho_L} \right) e^{-r^m_n \frac{z - z_0}{\rho_L}} \text{ for } \mathbf{r} \in \Omega_2 \tag{34}$$

and $\forall\left(n', m'\right)$, where the sign in the exponent of the z-variable provides the desirable ascendant behavior of the potential field Φ_c, as we suppose that it is directed upwards for the purposes of this work. Consequently, we multiply (34) by $\rho J_n \left(r^{\overline{m}}_n \frac{\rho}{\rho_L} \right) e^{-\mathrm{i}\overline{n}\varphi} y_{n/m} \left(z \right)$ for $\mathbf{r} \in \Omega_2$, integrating in the sequel over the main intervals of the variables and using the orthogonality relations (21) and (23), to recover the constants

$$A^{n'/m'}_{n/m} = \frac{\int_0^{z_0} \int_0^{2\pi} \int_0^{\rho_L} \left[U^{(\mathrm{ex})}_{n'/m'} \left(R, \hat{\mathbf{r}} \right) \right] J_n \left(r^m_n \frac{\rho}{\rho_L} \right) e^{-\mathrm{i}n\varphi} y_{n/m} \left(z \right) \rho \mathrm{d}\rho \mathrm{d}\varphi \mathrm{d}z}{\pi \rho_L^2 \left[J_{n+1} \left(r^m_n \right) \right]^2 \left\{ \int_0^{z_0} y_{n/m} \left(z \right) e^{-r^m_n \frac{z - z_0}{\rho_L}} \mathrm{d}z \right\}}, \tag{35}$$

where $n \in \mathbb{N}$, $m \in \mathbb{N}^*_+$, and $\forall\left(n', m'\right)$, while $y_{n/m}$ is a convenient function, actually being an arbitrary weighting function of integration over z-variable, appropriately chosen for simplifying integrals in (35) with respect to the inclusion's geometry. Although, the last difficulty to overcome is to adjust $\mathbf{r} \equiv (R, \hat{\mathbf{r}})$ inside (35) to the cylindrical coordinate system. Then, upon the use of a standard geometry for which the exterior eigenfunctions (27) attain a particular structure, the constants (35) can be computed. Once done, the corresponding potential Φ_c yields the complicated, yet similar to potential expressions (18) to (20), cylindrical expansion

$$\Phi_c \left(\mathbf{r} \right) = \sum_{n=-\infty}^{+\infty} e^{\mathrm{i}n\varphi} \sum_{m=1}^{+\infty} \left[\sum_{n'} \sum_{m'} A^{n'/m'}_{n/m} C^{(c)}_{n'/m'} \right] J_n \left(r^m_n \frac{\rho}{\rho_L} \right) e^{-r^m_n \frac{z - z_0}{\rho_L}} \text{ for } \mathbf{r} \in \Omega_2, \tag{36}$$

in terms of the known constants $A_{n/m}^{n'/m'}$ and the constant coefficients under evaluation $C_{n'/m'}^{(c)}$ for every $n \in \mathbb{N}$, $m \in \mathbb{N}_+^*$, and $\forall \left(n', m'\right)$. Continuing to the general-type conditions (32) and (33), we observe that potential Φ_f, provided by (20), is involved only with the cylindrical interior harmonics $J_n\left(r_n^m \frac{\rho}{\rho_L}\right) e^{\mathrm{in}\varphi} e^{r_n^m \frac{z-z_0}{\rho_L}}$ for $n \in \mathbb{N}$ and $m \in \mathbb{N}_+^*$, which are the solutions that must be expanded to the corresponding interior general basis. Therein,

$$J_n\left(r_n^m \frac{\rho}{\rho_L}\right) e^{\mathrm{in}\varphi} e^{r_n^m \frac{z-z_0}{\rho_L}} = \sum_{n'} \sum_{m'} B_{n'/m'}^{n/m} U_{n'/m'}^{(\mathrm{in})}(\mathbf{r}) \equiv \sum_{n'} \sum_{m'} B_{n'/m'}^{n/m} G_{n'/m'}^{(\mathrm{in})}(R)\, g_{n'/m'}(\hat{\mathbf{r}}) \text{ for } \mathbf{r} \in \Omega_2 \tag{37}$$

and for $n \in \mathbb{N}$ and $m \in \mathbb{N}_+^*$, where the choice of the interior general eigenfunctions coincides with the demanding descendant behavior of the potential field Φ_f, as we presume that it is directed downwards in this study. Therefore, we may multiply (37) by $x_{n'/m'}(R)\, h(\hat{\mathbf{r}})\, \overline{g}_{n'/m'}(\hat{\mathbf{r}})$ for every $\mathbf{r} \in \Omega_2$ and afterwards integrate over the main intervals of the variables, where utilizing the orthogonality relation (28), we reach to the constants

$$B_{n'/m'}^{n/m} = \frac{\int_{R_v}^{R_L} \iint_{S_v} \left[J_n\left(r_n^m \frac{\rho}{\rho_L}\right) e^{\mathrm{in}\varphi} e^{r_n^m \frac{z-z_0}{\rho_L}}\right] x_{n'/m'}(R)\, h(\hat{\mathbf{r}})\, \overline{g}_{n'/m'}(\hat{\mathbf{r}})\, \mathrm{d}S(\hat{\mathbf{r}})\, \mathrm{d}R}{\mathrm{d}_{n'/m'} \left\{\int_{R_v}^{R_L} G_{n'/m'}^{(\mathrm{in})}(R)\, x_{n'/m'}(R)\, \mathrm{d}R\right\}}, \tag{38}$$

where $\forall \left(n', m'\right)$ with $n \in \mathbb{N}$ and $m \in \mathbb{N}_+^*$, while $x_{n',m'}$ is a function of practical interest, being in fact an arbitrary weighting function for integration over R-variable, conveniently chosen for simplifying integrals within (38) with respect to a specific geometry of the inclusion. Nevertheless, the final difficultness to exceed is to write the position vector $\mathbf{r} \equiv (\rho, \varphi, z)$ into (38) for a particular implied geometry, whereas the interior eigenfunctions (26) have a standard form and the constants (38) can be calculated. Eventually, the corresponding potential Φ_f yields the complicated, yet similar to (24) and (25) with (26) and (27), general expansion

$$\Phi_f(\mathbf{r}) = \sum_{n'} \sum_{m'} \left[\sum_{n=-\infty}^{+\infty} \sum_{m=1}^{+\infty} B_{n'/m'}^{n/m} C_{n/m}^{(f)}\right] G_{n'/m'}^{(\mathrm{in})}(R)\, g_{n'/m'}(\hat{\mathbf{r}}) \text{ for } \mathbf{r} \in \Omega_2 \tag{39}$$

in view of the known constants $B_{n'/m'}^{n/m}$ and the constant coefficients under evaluation $C_{n/m}^{(f)}$ for $\forall \left(n', m'\right)$ with $n \in \mathbb{N}$ and $m \in \mathbb{N}_+^*$.

The aforementioned procedure is the key to our analytical method, which is based on producing integral representations of ready-to-use formulae in terms of well-known eigenfuctions. Thus, the harmonic potentials, which are involved with the continuity conditions (30) to (33), are properly configured to fit both their cylindrical and general aspect in the weak sense. In the sequel, we proceed as follows. We primarily substitute the potential functions (18) to (20) and the cylindrical-type one from (36) into the first set of conditions on the plane interface for $z = z_0$, ie, (30) and (31), where applying orthogonality rules based on (21) and (23), we obtain the corresponding first set of equations for the unknown constant coefficients, ie,

$$\sum_{n'} \sum_{m'} A_{n/m}^{n'/m'} C_{n'/m'}^{(c)} + C_{n/m}^{(f)} - \mu_r C_{n/m}^{(a)} = \mu_r C_{n/m}^{(s)} \text{ for every } n \in \mathbb{N} \text{ and } m \in \mathbb{N}_+^*, \tag{40}$$

while

$$\sum_{n'} \sum_{m'} A_{n/m}^{n'/m'} C_{n'/m'}^{(c)} - C_{n/m}^{(f)} - C_{n/m}^{(a)} = -C_{n/m}^{(s)} \text{ for every } n \in \mathbb{N} \text{ and } m \in \mathbb{N}_+^*, \tag{41}$$

where (40) and (41) are linear algebraic equations. In the second place, we substitute the potential functions (24) and (25), along with the general-type one from (39) into the second set of conditions on the arbitrary interface between the inclusion and the ferromagnetic medium at $R = R_v$, ie, (32) and (33), where applying orthogonality rules with regard to (28), we conclude to the corresponding second set of equations for the constant coefficients, given by

$$\sum_{n=-\infty}^{+\infty} \sum_{m=1}^{+\infty} B_{n'/m'}^{n/m} C_{n/m}^{(f)} + \frac{G_{n'/m'}^{(\mathrm{ex})}(R_v)}{G_{n'/m'}^{(\mathrm{in})}(R_v)} C_{n'/m'}^{(c)} - \mu_r C_{n'/m'}^{(v)} = 0 \text{ for every } \forall \left(n', m'\right) \tag{42}$$

and

$$\sum_{n=-\infty}^{+\infty} \sum_{m=1}^{+\infty} B_{n'/m'}^{n/m} C_{n/m}^{(f)} + \frac{G_{n'/m'}^{(\mathrm{ex})'}(R_v)}{G_{n'/m'}^{(\mathrm{in})'}(R_v)} C_{n'/m'}^{(c)} - C_{n'/m'}^{(v)} = 0 \text{ for every } \forall \left(n', m'\right), \tag{43}$$

where (42) and (43) are linear algebraic equations as well, while the prime denotes differentiation with respect to the argument. Relationships (40) to (43) can be manipulated further, and after some algebra, we reach the following closed-type and ready-to-use form relations

$$C_{n/m}^{(a)} = \frac{1}{\mu_r - 1}\left[2C_{n/m}^{(f)} - (\mu_r + 1)\, C_{n/m}^{(s)}\right] \text{ for every } n \in \mathbb{N} \text{ and } m \in \mathbb{N}_+^* \tag{44}$$

and

$$C_{n'/m'}^{(v)} = \frac{1}{\mu_r - 1}\left[\frac{G_{n'/m'}^{(\mathrm{ex})}(R_v)}{G_{n'/m'}^{(\mathrm{in})}(R_v)} - \frac{G_{n'/m'}^{(\mathrm{ex})'}(R_v)}{G_{n'/m'}^{(\mathrm{in})'}(R_v)}\right] C_{n'/m'}^{(c)} \text{ for every } \forall\left(n', m'\right), \tag{45}$$

providing in an analytical fashion $C_{n/m}^{(a)}$ and $C_{n'/m'}^{(v)}$, once $C_{n/m}^{(f)}$ and $C_{n'/m'}^{(c)}$ are evaluated, respectively, since $C_{n/m}^{(s)}$ is the acquainted coefficient that corresponds to the current coil for $n \in \mathbb{N}$, $m \in \mathbb{N}_+^*$ and $\forall\left(n', m'\right)$. Those are the unknown constant coefficients that are combined with the transmitted term from the plane interface and the reflection from the inclusion, satisfying

$$C_{n/m}^{(f)} = \frac{1}{\mu_r + 1}\left[2\mu_r C_{n/m}^{(s)} + (\mu_r - 1)\sum_{n'}\sum_{m'} A_{n/m}^{n'/m'} C_{n'/m'}^{(c)}\right] \text{ for every } n \in \mathbb{N} \text{ and } m \in \mathbb{N}_+^* \tag{46}$$

and

$$C_{n'/m'}^{(c)} = (\mu_r - 1)\left[\frac{G_{n'/m'}^{(\mathrm{ex})}(R_v)}{G_{n'/m'}^{(\mathrm{in})}(R_v)} - \mu_r \frac{G_{n'/m'}^{(\mathrm{ex})'}(R_v)}{G_{n'/m'}^{(\mathrm{in})'}(R_v)}\right]^{-1} \sum_{n=-\infty}^{+\infty}\sum_{m=1}^{+\infty} B_{n'/m'}^{n/m} C_{n/m}^{(f)} \text{ for every } \forall\left(n', m'\right), \tag{47}$$

respectively. Relationships (46) and (47) comprise a set of intertwined equations with respect to $C_{n/m}^{(f)}$ and $C_{n'/m'}^{(c)}$, since $C_{n/m}^{(s)}$ is well known, while the constants $A_{n/m}^{n'/m'}$ and $B_{n'/m'}^{n/m}$ come from (35) and (38), respectively, all for every $n \in \mathbb{N}$, $m \in \mathbb{N}_+^*$, and $\forall\left(n', m'\right)$. In fact, they are standard systems of linear algebraic equations and they can be solved with cut-off techniques so as to obtain the aforementioned unknown constant coefficients via an easy computational technique for the solution of the linear systems. Although, one could proceed one step further and substitute (47) into (46), leading to

$$\begin{aligned}\sum_{n'}\sum_{m'} A_{n/m}^{n'/m'}\left[\mu_r \frac{G_{n'/m'}^{(\mathrm{ex})'}(R_v)}{G_{n'/m'}^{(\mathrm{in})'}(R_v)} - \frac{G_{n'/m'}^{(\mathrm{ex})}(R_v)}{G_{n'/m'}^{(\mathrm{in})}(R_v)}\right]^{-1} \sum_{N=-\infty}^{+\infty}\sum_{M=1}^{+\infty} B_{n'/m'}^{N/M} C_{N/M}^{(f)} + \frac{\mu_r + 1}{(\mu_r - 1)^2} C_{n/m}^{(f)} \\ = \frac{2\mu_r}{(\mu_r - 1)^2} C_{n/m}^{(s)} \text{ for every } n \in \mathbb{N} \text{ and } m \in \mathbb{N}_+^*,\end{aligned} \tag{48}$$

after a necessary index interchange; hence, (46) is replaced by (48), whereas it consists of only one set of undetermined constants, those being the $C_{n/m}^{(f)}$ for $n \in \mathbb{N}$ and $m \in \mathbb{N}_+^*$. The idea is, when one of the applicable geometries (sphere, spheroid, ellipsoid, etc) is chosen to model the flaw into the ferromagnetic material, then all known constants and functions involved in (44) to (46) or (48) and (47) take specific values accordingly to the implied coordinate system. Then, the four sets of unknown constant coefficients $C_{n/m}^{(a)}$ and $C_{n/m}^{(f)}$ for $n \in \mathbb{N}$ and $m \in \mathbb{N}_+^*$, and $C_{n'/m'}^{(c)}$ and $C_{n'/m'}^{(v)}$ for $\forall\left(n', m'\right)$, given $C_{n/m}^{(s)}$ for $n \in \mathbb{N}$ and $m \in \mathbb{N}_+^*$ of the applied field, are readily recovered by the four sets of conditions, discussed earlier, as long as a proper truncation of the infinite series is used to obtain the desired accuracy. Therefore, our problem is solved in a way, as much general and analytical as possible. Thereafter, the incorporated potentials, ie, Φ_s, Φ_a, and Φ_f via (18) to (20), and Φ_c and Φ_v through (24) and (25) with the aid of (26) and (27), are instantly obtained, while the magnetostatic vector fields within the different domains of interest read

$$\mathbf{B}_1(\mathbf{r}) = -\nabla\left[\Phi_s(\mathbf{r}) + \Phi_a(\mathbf{r})\right] \text{ with } \nabla\cdot\mathbf{B}_1(\mathbf{r}) = 0 \text{ for } \mathbf{r} \in \Omega_1 \tag{49}$$

$$\mathbf{B}_2(\mathbf{r}) = -\nabla\left[\Phi_f(\mathbf{r}) + \Phi_c(\mathbf{r})\right] \text{ with } \nabla\cdot\mathbf{B}_2(\mathbf{r}) = 0 \text{ for } \mathbf{r} \in \Omega_2 \tag{50}$$

and

$$\mathbf{B}_v(\mathbf{r}) = -\nabla\Phi_v(\mathbf{r}) \text{ with } \nabla\cdot\mathbf{B}_1(\mathbf{r}) = 0 \text{ for } \mathbf{r} \in \Omega_v, \tag{51}$$

reaching our final goal. The crucial issue in this method is the evaluation of the integrals that appear within the numerators of (35) and (38) if a well-fitted geometry represents the shape of a possible inclusion. Even though our primary concern is to push as far as possible the analytical manipulation of these integrals, the imposition of a numerical procedure at some point is inevitable, depending on the complexity of the utilized coordinate system and the eigenfunctions

associated with it. The efficiency of the analytical tools is to be demonstrated in the forthcoming section, where, as an application, the inclusion is considered spherical.

4 - ANALYTICAL APPLICATION FOR A SPHERICAL INCLUSION

In order to illustrate our semianalytical approach, we address a particular geometrical characteristic of the void inclusion, resembling a spherical defect. We assume that the center of the reference cylindrical coordinate system coincides with the center of the sphere at $(0,0,0)$, while the orientation does not affect the analysis, since the sphere represents the complete isotropy of the 3-D space. Herein, the corresponding boundary value problem becomes specific and all the introduced quantities, interconnected with the inclusion's geometry in the theoretical analysis, are adjusted now in the spherical coordinate regime. Thus, any connection of variables, vector or scalar functions, and other parameters with the general case will be designated by referring to the general notation used in the previous section.

At this point, in order to make this work complete and independent, we invoke some useful information relative to the spherical geometry. In more details, we formulate the problem with respect to a sphere-shaped inclusion of fixed radius r_s, which is the characteristic variable of the inclusion's surface, ie, $R_v \equiv r_s$. The radial spherical variable $r \in [0, +\infty)$ denotes the spatial characteristic variable, ie, $R \equiv r$, pointing either inside for $r \in [0, r_s)$ or outside for any $r \in (r_s, r_L]$ the sphere, r_L being the characteristic spherical variable that corresponds to the cylindrical area opening for $\rho = \rho_L$, appointing $R_L \equiv r_L$, while the angular dependence comes from $\zeta \equiv \cos\theta \in [-1,1]$ and $\phi \in [0, 2\pi)$ (actually $\phi = \varphi$ in our case). In terms of these variables, we define the implemented to our application spherical coordinate system via

$$\mathbf{r} = (r, \zeta, \phi) = r\zeta\hat{\boldsymbol{x}}_1 + r\sqrt{1-\zeta^2}\cos\phi\hat{\boldsymbol{x}}_2 + r\sqrt{1-\zeta^2}\sin\phi\hat{\boldsymbol{x}}_3 = r\hat{\boldsymbol{r}}, \tag{52}$$

in terms of the Cartesian basis, where the unit normal coordinate vectors of this system $\hat{\boldsymbol{r}}$, $\hat{\boldsymbol{\zeta}}$, and $\hat{\boldsymbol{\phi}}$, as written to denote the (r, ζ, ϕ) clockwise system, assume the forms

$$\hat{\boldsymbol{r}} = \zeta\hat{\boldsymbol{x}}_1 + \sqrt{1-\zeta^2}\cos\phi\hat{\boldsymbol{x}}_2 + \sqrt{1-\zeta^2}\sin\phi\hat{\boldsymbol{x}}_3 \equiv \hat{\boldsymbol{n}}_s, \tag{53}$$

which matches the outward pointing unit normal vector $\hat{\boldsymbol{n}}_s$ on the surface of the spherical inclusion, while

$$\hat{\boldsymbol{\zeta}} = \sqrt{1-\zeta^2}\hat{\boldsymbol{x}}_1 - \zeta\cos\phi\hat{\boldsymbol{x}}_2 - \zeta\sin\phi\hat{\boldsymbol{x}}_3 \text{ and } \hat{\boldsymbol{\phi}} = -\sin\phi\hat{\boldsymbol{x}}_2 + \cos\phi\hat{\boldsymbol{x}}_3 = \hat{\boldsymbol{\varphi}}. \tag{54}$$

In fact, to be consistent with our generalized technique, $\hat{\boldsymbol{n}} \equiv \hat{\boldsymbol{n}}_s$ or $\hat{\boldsymbol{R}} \equiv \hat{\boldsymbol{r}}$, while $\hat{\mathbf{r}} \equiv (\zeta, \phi)$ for $\zeta \in [-1,1]$ and $\phi \in [0, 2\pi)$.

The gradient and the Laplacian operators yield

$$\nabla' = \hat{\boldsymbol{r}}\frac{\partial}{\partial r} + \frac{1}{r}\boldsymbol{D}_s(\hat{\boldsymbol{r}}), \text{where } \boldsymbol{D}_s(\hat{\boldsymbol{r}}) = -\sqrt{1-\zeta^2}\hat{\boldsymbol{\zeta}}\frac{\partial}{\partial\zeta} + \frac{1}{\sqrt{1-\zeta^2}}\hat{\boldsymbol{\phi}}\frac{\partial}{\partial\phi} \tag{55}$$

and

$$\Delta' = \frac{1}{r^2}\frac{\partial}{\partial r}\left(r^2\frac{\partial}{\partial r}\right) + \frac{1}{r^2}\frac{\partial}{\partial\zeta}\left(\left(1-\zeta^2\right)\frac{\partial}{\partial\zeta}\right) + \frac{1}{r^2\left(1-\zeta^2\right)}\frac{\partial^2}{\partial\phi^2}, \tag{56}$$

respectively, for every $r \in [0, r_s)$, $\zeta \in [-1,1]$ and $\phi \in [0, 2\pi)$, while it is obvious that the matching $\boldsymbol{D}(\hat{\mathbf{r}}; R) \equiv \boldsymbol{D}_s(\hat{\boldsymbol{r}})$ and $Q(R; \hat{\mathbf{r}}) \equiv 1$ certifies (55) from (29). On the other hand, completing this trivial but necessary analysis for the purposes of reducing the general case to this application, the interior spatial domain of the spherical inclusion admits

$$\Omega_s = \left\{(r, \zeta, \phi), \in \mathbb{R}^3 : r \in [0, r_s), \zeta \in [-1,1], \phi \in [0, 2\pi)\right\} \subset \Omega, \tag{57}$$

as a subset of the entire domain Ω, while the spherical-type surface is secured by the simply connected set

$$S_s = \left\{(r_s, \zeta, \phi) \in \mathbb{R}^3 : \zeta \in [-1,1], \phi \in [0, 2\pi)\right\}, \tag{58}$$

whereas (57) and (58) imply $\Omega_v \equiv \Omega_s$ and $S_v \equiv S_s$. Here, we must clarify that the cylindrical-type domain outside the spherical inclusion Ω_2 remains unaltered. However, special care is needed for the spherical functions associated with Ω_2. Hence, the physical problem that we are about to solve is mathematically adjusted to the aforementioned introduced spherical geometry.

Aiming now to clarify the passage of the performed analysis from the general arbitrary case to the spherical one, we act as follows. Any function that belongs to the kernel space of the Laplace's operator (56) is written in terms of the interior (regular at the origin) and the exterior (regular at infinity) spherical harmonic eigenfunctions

$$U^{(\text{in})}_{n'/m'}(\mathbf{r}) \equiv r^{n'}Y^{m'}_{n'}(\zeta, \phi) \text{ for } \mathbf{r} \in \Omega_s \text{ and } U^{(\text{ex})}_{n'/m'}(\mathbf{r}) \equiv r^{-(n'+1)}Y^{m'}_{n'}(\zeta, \phi) \text{ for } \mathbf{r} \in \Omega_2, \tag{59}$$

respectively, as a function of the surface spherical harmonics $Y_{n'}^{m'}$, where the convenient symbolism "$\forall(n', m')$" is from now on replaced by the corresponding intervals for our case, ie, $n' \geq 0$ and $|m'| \leq n'$, to obtain the required number of $2n'+1$ spherical eigenfunctions. By virtue of (59) and the general definitions (26) and (27), the radial dependence merges $G_{n'/m'}^{(\mathrm{in})}(R) \equiv r^{n'}$ for any $r < r_s$ and $G_{n'/m'}^{(\mathrm{ex})}(R) \equiv r^{-(n'+1)}$ at $r_s < r < r_L$, while the common angular dependence reveals that $g_{n'/m'}(\hat{\mathbf{r}}) \equiv Y_{n'}^{m'}(\zeta, \phi)$. The surface spherical harmonics and their conjugate form are defined as

$$Y_{n'}^{m'}(\zeta,\phi) = P_{n'}^{m'}(\zeta)e^{im'\phi} \text{ and } Y_{n'}^{m'*}(\zeta,\phi) = P_{n'}^{m'}(\zeta)e^{-im'\phi} \equiv (-1)^{|m'|}Y_{n'}^{-|m'|}(\zeta,\phi) \text{ for } (\zeta,\phi) \in S_s \tag{60}$$

with $n' \geq 0$ and $|m'| \leq n'$, provided as a function of the well-known associated Legendre functions of the first kind

$$P_{n'}^{m'}(\zeta) = \frac{1}{2^{n'}n'!}\left(1-\zeta^2\right)^{|m'|/2}\frac{d^{n'+|m'|}}{d\zeta^{n'+|m'|}}\left(\zeta^2-1\right)^{n'} \text{ for } |\zeta| \leq 1 \text{ with } n' \geq 0 \text{ and } \left|m'\right| \leq n', \tag{61}$$

which are regular when $\zeta = \pm 1$. However, functions $Y_{n'}^{m'}$ are orthogonal with respect to the surface relation on S_s and on any spherical surface of constant radius, yielding

$$\int_0^{2\pi}\int_{-1}^{+1} Y_{n'}^{m'}(\zeta,\phi)Y_{\overline{n}'}^{\overline{m}'*}(\zeta,\phi)\mathrm{d}\zeta\mathrm{d}\phi = \frac{4\pi}{2n'+1}\frac{(n'+|m'|)!}{(n'-|m'|)!}\delta_{n'\overline{n}'}\delta_{m'\overline{m}'}, \tag{62}$$

in view of Kronecker's deltas. Integral (62) is the analogous of the general orthogonality relationship (28) if we set $h(\hat{\mathbf{r}}) \equiv 1$, $d_{n'/m'} \equiv \frac{4\pi}{2n'+1}\frac{(n'+|m'|)!}{(n'-|m'|)!}$ as aforementioned; since it holds $g_{n'/m'}(\hat{\mathbf{r}}) \equiv Y_{n'}^{m'}(\zeta,\phi)$, then $\overline{g}_{\overline{n'}/\overline{m'}}(\hat{\mathbf{r}}) \equiv Y_{\overline{n}'}^{\overline{m}'*}(\zeta,\phi)$. Therefore, with respect to the present analysis, the harmonic potentials Φ_c and Φ_v, which are associated with the inclusion and given by the general expansions (24) and (25), respectively, inherit the spherical description of the current application and provide us with

$$\Phi_c(\mathbf{r}) = \sum_{n'=0}^{+\infty}\sum_{m'=-n'}^{n'} C_{n'/m'}^{(c)} r^{-(n'+1)} Y_{n'}^{m'}(\zeta,\phi) \text{ for every } \mathbf{r} \in \Omega_2 \tag{63}$$

and

$$\Phi_v(\mathbf{r}) = \sum_{n'=0}^{+\infty}\sum_{m'=-n'}^{n'} C_{n'/m'}^{(v)} r^{n'} Y_{n'}^{m'}(\zeta,\phi) \text{ for every } \mathbf{r} \in \Omega_s, \tag{64}$$

following the spherical harmonic analysis, whereas for the domain Ω_2, we are obliged to convert the variables from the cylindrical to the spherical coordinates. On the other hand, the potentials associated with the cylindrical domains satisfy (18) to (20).

In the sequel and under the aim to demonstrate the theoretical analysis, we proceed directly to the results for a general shaped inclusion and specifically to the calculation of the unknown constant coefficients in between (44) and (48). Substituting all the transformation relations discussed herein to (44) to (48), those are reduced as follows, ie, (44) remains unaltered, so as to give

$$C_{n/m}^{(a)} = \frac{1}{\mu_r - 1}\left[2C_{n/m}^{(f)} - (\mu_r+1)C_{n/m}^{(s)}\right] \text{ for every } n \in \mathbb{N} \text{ and } m \in \mathbb{N}_+^*, \tag{65}$$

and (45) becomes

$$C_{n'/m'}^{(v)} = \frac{2n'+1}{n'(\mu_r-1)r_s^{2n'+1}}C_{n'/m'}^{(c)} \text{ for every } n' \geq 0 \text{ and } \left|m'\right| \leq n', \tag{66}$$

where the particular case for $n' = m' = 0$ arises also from (66), giving $C_{0/0}^{(c)} = 0$ and $C_{0/0}^{(v)} \in \mathbb{R}$ is an arbitrarily chosen constant, which does not contribute at all to the final magnetostatic field, since it corresponds to the constant part of potential (64) that vanishes under the gradient action. Hence, we may choose $C_{0/0}^{(v)} \equiv 0$, without loss of the consistency and the generality of our results. Relation (46) is not affected, ie,

$$C_{n/m}^{(f)} = \frac{1}{\mu_r+1}\left[2\mu_r C_{n/m}^{(s)} + (\mu_r-1)\sum_{n'=0}^{+\infty}\sum_{m'=-n'}^{n'} A_{n/m}^{n'/m'}C_{n'/m'}^{(c)}\right] \text{ for every } n \in \mathbb{N} \text{ and } m \in \mathbb{N}_+^*, \tag{67}$$

while similar argumentation for (47) leads to

$$C_{n'/m'}^{(c)} = \frac{n'(\mu_r-1)r_s^{2n'+1}}{n'(\mu_r+1)+\mu_r}\sum_{n=-\infty}^{+\infty}\sum_{m=1}^{+\infty} B_{n'/m'}^{n/m}C_{n/m}^{(f)} \text{ for every } n' \geq 0 \text{ and } \left|m'\right| \leq n', \tag{68}$$

which, by virtue of (67) (see directly (48) for instance), renders

$$\sum_{n'=0}^{+\infty}\sum_{m'=-n'}^{n'} A_{n/m}^{n'/m'}\left[\frac{n' r_s^{2n'+1}}{n'(\mu_r+1)+\mu_r}\right]\sum_{N=-\infty}^{+\infty}\sum_{M=1}^{+\infty} B_{n'/m'}^{N/M} C_{N/M}^{(f)} - \frac{\mu_r+1}{(\mu_r-1)^2} C_{n/m}^{(f)} = -\frac{2\mu_r}{(\mu_r-1)^2} C_{n/m}^{(s)} \tag{69}$$

for every $n \in \mathbb{N}$ and $m \in \mathbb{N}_+^*$, where $C_{n/m}^{(s)}$ refers to applied source field of the current coil for every $n \in \mathbb{N}$ and $m \in \mathbb{N}_+^*$. Our final task is to convert the known constants $A_{n/m}^{n'/m'}$ and $B_{n'/m'}^{n/m}$ from (35) and (38), respectively, for any $n \in \mathbb{N}$ and $m \in \mathbb{N}_+^*$, as well for any $n' \geq 0$ and $|m'| \leq n'$ to the corresponding spherical constants. If we consider that $\phi = \varphi$, both belonging to $[0, 2\pi)$, then with respect to the azimuthal angular orthogonality relation (23), we recover the following handy expressions in terms of easy-to-handle functions that remain bounded within the integration intervals, ie,

$$A_{n/m}^{n'/m'} = \frac{2\delta_{m'n}\int_0^{z_0}\int_0^{\rho_L}\left[r^{-(n'+1)}P_{n'}^{m'}(\zeta)\right]\rho J_n\left(r_n^m\frac{\rho}{\rho_L}\right)y_{n/m}(z)\,\mathrm{d}\rho\mathrm{d}z}{\rho_L^2\left[J_{n+1}\left(r_n^m\right)\right]^2\left\{\int_0^{z_0} y_{n/m}(z)\,e^{-r_n^m\frac{z-z_0}{\rho_L}}\mathrm{d}z\right\}} \tag{70}$$

and

$$B_{n'/m'}^{n/m} = \frac{\left(2n'+1\right)\left(n'-|m'|\right)!\delta_{nm'}\int_{r_s}^{r_L}\int_{-1}^{+1}\left[J_n\left(r_n^m\frac{\rho}{\rho_L}\right)e^{r_n^m\frac{z-z_0}{\rho_L}}\right]x_{n'/m'}(r)\,P_{n'}^{m'}(\zeta)\,\mathrm{d}\zeta\mathrm{d}r}{2\left(n'+|m'|\right)!\left\{\int_{r_s}^{r_L} r^{n'}x_{n'/m'}(r)\,\mathrm{d}r\right\}}, \tag{71}$$

whereas the quantity $r^{-(n'+1)}P_{n'}^{m'}(\zeta)$ into (70) must be represented in terms of the cylindrical variables (ρ, z), while $J_n\left(r_n^m\frac{\rho}{\rho_L}\right)e^{r_n^m\frac{z-z_0}{\rho_L}}$ within (71) should admit spherical behavior under the (r, ζ) dependence. This is feasible by means of the relations $\rho = r\sqrt{1-\zeta^2}$ and $z = r\zeta$, which are the outcome of matching (2) with (52). Let us recall that $y_{n/m}(z)$ for $z \in [0, z_0]$ with $n \in \mathbb{N}$ and $m \in \mathbb{N}_+^*$, and $x_{n'/m'}(r)$ for $r \in [r_s, r_L]$ with $n' \geq 0$ and $|m'| \leq n'$, provide us with the flexibility in evaluating (70) and (71).

An interesting result follows after further manipulation of (70) and (71), revealing that, since $\delta_{m'n} = \delta_{nm'} = 0$ when $n \neq m'$, then

$$A_{n/m}^{n'/m'} = B_{n'/m'}^{n/m} = 0 \text{ for } n \in \mathbb{N}, m \in \mathbb{N}_+^* \text{ and } n' \geq 0, \left|m'\right| \leq n' \text{ with } n \neq m', \tag{72}$$

forcing the constant coefficients (66) and (68) to vanish, ie,

$$C_{n'/m'}^{(v)}\Big|_{n\neq m'} = C_{n'/m'}^{(c)}\Big|_{n\neq m'} = 0 \text{ for every } n' \geq 0 \text{ and } \left|m'\right| \leq n', \tag{73}$$

while the remaining constant coefficients (65) and (67) yield

$$C_{n/m}^{(a)}\Big|_{n\neq m'} = -\frac{\mu_r-1}{\mu_r+1}C_{n/m}^{(s)} \text{ and } C_{n/m}^{(f)}\Big|_{n\neq m'} = \frac{2\mu_r}{\mu_r+1}C_{n/m}^{(s)} \text{ for every } n \in \mathbb{N} \text{ and } m \in \mathbb{N}_+^*, \tag{74}$$

in terms of the exerted field's constant coefficients $C_{n/m}^{(s)}$ for $n \in \mathbb{N}$ and $m \in \mathbb{N}_+^*$. The results (73) and (74) reflect the absence of any field either inside the inclusion (see, for instance, (64) to verify $\Phi_v|_{n\neq m'} = 0$) or reflected by the void (see, similarly, (63), showing $\Phi_c|_{n\neq m'} = 0$). On the other hand, the surviving potentials (19) and (20), associated with the planar interface, are written suitably by substitution of (74), as

$$\Phi_a(\mathbf{r})|_{n\neq m'} = -\frac{\mu_r-1}{\mu_r+1}\sum_{n=-\infty}^{+\infty} e^{\mathrm{i}n\varphi}\sum_{m=1}^{+\infty} C_{n/m}^{(s)} J_n\left(r_n^m\frac{\rho}{\rho_L}\right)e^{-r_n^m\frac{z-z_0}{\rho_L}} \text{ for } \mathbf{r} \in \Omega_1 \tag{75}$$

and

$$\Phi_f(\mathbf{r})|_{n\neq m'} = \frac{2\mu_r}{\mu_r+1}\sum_{n=-\infty}^{+\infty} e^{\mathrm{i}n\varphi}\sum_{m=1}^{+\infty} C_{n/m}^{(s)} J_n\left(r_n^m\frac{\rho}{\rho_L}\right)e^{r_n^m\frac{z-z_0}{\rho_L}} \text{ for } \mathbf{r} \in \Omega_2, \tag{76}$$

once (18) is invoked, while the related magnetostatic fields assume $\mathbf{B}_a|_{n\neq m'} = -\nabla\Phi_a|_{n\neq m'}$ and $\mathbf{B}_f\big|_{n\neq m'} = -\nabla\Phi_f\big|_{n\neq m'}$, whereas $\mathbf{B}_s|_{n\neq m'} = -\nabla\Phi_s|_{n\neq m'}$ is the prescribed incident magnetostatic field. Obviously, this case resembles the special physical problem, where there is no inclusion; hence, we actually deal with a simple transmission problem between air

and ferromagnetic media with current coil excitation. However, the discussed case where $n \neq m'$ must not be confused with the also interesting limiting case, whereas the radius of the spherical inclusion tends to zero ($r_s \to 0$), because, in this particular occasion, the inclusion is not absent but exists as a singularity point without dimensions within the ferromagnetic medium. Herein, a careful, though trivial, limiting procedure has to be followed for the spherical results, which is based strictly to the choice of function $x_{n'/m'}(r)$ for every $r \in [r_s, r_L]$ with $n' \geq 0$ and $|m'| \leq n'$ into (71), since it will provide us with appropriate dependence upon r_s.

Recapitulating the completely analytical elaboration of the spherical inclusion problem, we mention that once the integrals appearing within (70) and (71) are computed; then, the related expansion constants are calculated and when they are readily inserted into relationships (65) to (68) (or instead (68), pose (69) alternatively), we end up with systems of linear algebraic equations. These can be solved with usual cut-off computational techniques so as to obtain the unknown constant coefficients $C^{(a)}_{n/m}$ and $C^{(f)}_{n/m}$ for $n \in \mathbb{N}$ and $m \in \mathbb{N}^*_+$, and $C^{(c)}_{n'/m'}$ and $C^{(v)}_{n'/m'}$ for $n' \geq 0$ and $|m'| \leq n'$, given $C^{(s)}_{n/m}$ for $n \in \mathbb{N}$ and $m \in \mathbb{N}^*_+$. When accuracy is achieved, the interrelated potentials Φ_s, Φ_a, and Φ_f via (18) to (20), and Φ_c and Φ_v through (24) and (25) with the aid of (26) and (27), are immediately settled, while the magnetostatic vector fields arise from (49) to (51) for the demonstrated situation, where the domain of the inclusion has been considered spherical.

As it was intensively discussed, the crucial threshold of the succession of our method is the evaluation of the integrals that appear within (70) and (71), since all the information about the inclusion's geometry is embedded in these conversion formulae. Besides, the solution of the system of linear equations (65) to (68) that will yield the sought development coefficients is an easy task, considering the facility of solving such systems. To this end, we attempt to precede the analysis a few steps further and seek the conversion relations from exterior spherical functions to cylindrical ones and from cylindrical to interior spherical modes, namely,

$$r^{-(n'+1)} P^{m'}_{n'}(\zeta) = \sum_{m=1}^{+\infty} A^{n'/m'}_{m'/m} J_{m'}\left(r^m_{m'} \frac{\rho}{\rho_L}\right) e^{-r^m_{m'} \frac{z-z_0}{\rho_L}} = \sum_{m=1}^{+\infty} \left[A^{n'/m'}_{m'/m} e^{\left(r^m_{m'}/\rho_L\right) z_0}\right] J_{m'}\left(r^m_{m'} \frac{\rho}{\rho_L}\right) e^{-\left(r^m_{m'}/\rho_L\right) z} \tag{77}$$

with $n' \geq 0$ and $|m'| \leq n'$, while

$$J_n\left(r^m_n \frac{\rho}{\rho_L}\right) e^{r^m_n \frac{z-z_0}{\rho_L}} = \sum_{n'=0}^{+\infty} B^{n/m}_{n'/n} r^{n'} P^n_{n'}(\zeta) \text{ or } J_n\left(r^m_n \frac{\rho}{\rho_L}\right) e^{(r^m_n/\rho_L) z} = \sum_{n'=0}^{+\infty} \left[B^{n/m}_{n'/n} e^{(r^m_n/\rho_L) z_0}\right] r^{n'} P^n_{n'}(\zeta) \tag{78}$$

with $n \in \mathbb{N}$ and $m \in \mathbb{N}^*_+$, both (77) and (78) being valid at $\mathbf{r} \in \Omega_2$ and written suitably to refer to the origin, where we have kept only the terms for $n = m'$, which give nonzero constants (70) and (71), while the azimuthal dependence is omitted for reasons of clarity, since both the implied systems are rotational symmetric. Besides, this statement is readily proved, since the azimuthal angle lacks from the integrals in (70) and (71). As said, we have to determine the coefficients (70) and (71) to obtain the expansions (77) and (78) for $n = m'$.

We start with the conversion from the cylindrical to the external spherical eigenfunctions to produce expansion (77). We consider the identity

$$\int_0^{+\infty} e^{-x\cos\theta} J_{-q}(x\sin\theta)\, x^p \mathrm{d}x = \Gamma(p-q+1)\, P^q_p(\cos\theta) \text{ for } 0 < \theta < \frac{\pi}{2} \text{ and } \mathrm{Re}\left[p-q\right] > -1, \tag{79}$$

where the Gamma function Γ, given any complex number u with $\mathrm{Re}\, u > 0$, is provided by

$$\Gamma(u) = \int_0^{+\infty} e^{-t} t^{u-1} \mathrm{d}t = 2\int_0^{+\infty} e^{-t^2} t^{2u-1} \mathrm{d}t = \int_0^1 \ln^{u-1}\left(\frac{1}{t}\right) \mathrm{d}t \text{ with } \Gamma(u+1) = u\Gamma(u) \text{ and } \Gamma\left(\frac{1}{2}\right) = \sqrt{\pi}. \tag{80}$$

We make the convenient modifications into (79) by setting $\zeta = \cos\theta$, changing the integration variable $x \to \lambda r$, using the fact that $J_{-q} = (-1)^q J_q$, switching to cylindrical coordinates by means of the relations $\rho = r\sqrt{1-\zeta^2}$ and $z = r\zeta$, and putting together all the proper indexes as $p \to n'$ and $q \to m'$; thus, since $\Gamma(n'-m'+1) = (n'-m')!$, we arrive at

$$r^{-(n'+1)} P^{m'}_{n'}(\zeta) = \frac{(-1)^{m'}}{(n'-m')!} \int_0^{+\infty} \lambda^{n'} e^{-\lambda z} J_{m'}(\lambda\rho)\, \mathrm{d}\lambda \text{ for } \mathbf{r} \in \Omega_2 \text{ with } n' \geq 0 \text{ and } \left|m'\right| \leq n', \tag{81}$$

where the two constrains implied by (79) are fulfilled, noticing that $\mathrm{Re}[n'-m'] \equiv n'-m' > -1$. Finally, the demand of zero magnetostatic field at the truncation surface $\rho = \rho_L$ is interpreted so that the constant λ to be an eigenvalue and

obtain discrete rather than continuous values, ie, $\lambda \equiv \lambda_{m'}^{m} = r_{m'}^{m}/\rho_L$, where $r_{m'}^{m}$ is the m-root ($m \geq 1$) of order m' (note $|m'| \leq n'$ with $n' \geq 0$) of the Bessel functions of the first kind, meaning $J_{m'}\left(r_{m'}^{m}\right) = 0$. However, the conversion relation (81) in its continuous version is much trickier in manipulating to obtain the final expression upon summation over the discrete spectrum. In fact, it can be proved that one has to readapt the normalization coefficients, which are different for the continuous and the discrete case, yielding the multiplication of (81) by the factor $2\left(\rho_L/r_{m'}^{m}\right)\rho_L^{-2}J_{m'+1}^{-2}\left(r_{m'}^{m}\right)$. This is not a rigorous mathematical proof though but merely an engineering approximation. A strictly mathematical proof would require a limiting procedure, yet this is out of the scope of our analysis at this point, whose main purpose is to establish a handy formula for passing from the discrete to the continuous representation and vice versa. Consequently, the integral within (81) becomes infinite series with respect to the above statement and for $m \geq 1$, ie,

$$r^{-(n'+1)}P_{n'}^{m'}(\zeta) = \frac{2\left(\rho_L/r_{m'}^{m}\right)}{\rho_L^2 J_{m'+1}^2\left(r_{m'}^{m}\right)}\left[\frac{(-1)^{m'}}{(n'-m')!\rho_L^{n'}}\sum_{m=1}^{+\infty}\left(r_{m'}^{m}\right)^{n'}J_{m'}\left(r_{m'}^{m}\frac{\rho}{\rho_L}\right)e^{-\left(r_{m'}^{m}/\rho_L\right)z}\right] \text{ for } \mathbf{r}\in\Omega_2 \tag{82}$$

with $n' \geq 0$ and $|m'| \leq n'$. Direct comparison of (77) and (82) yields the constants

$$A_{m'/m}^{n'/m'} = \frac{2(-1)^{m'}}{(n'-m')!}\frac{\left(r_{m'}^{m}\right)^{n'-1}}{\rho_L^{n'+1}J_{m'+1}^2\left(r_{m'}^{m}\right)}e^{-\frac{r_{m'}^{m}}{\rho_L}z_0} \text{ for every value of } m\geq 1, n'\geq 0 \text{ and } \left|m'\right| \leq n', \tag{83}$$

which stands for the desired result that coincides with the result coming from (70) for the surviving constants if $n = m'$ with $|m'| \leq n'$ and $n' \geq 0$. We mention that restriction $\theta \in \left(0, \frac{\pi}{2}\right)$ in (79) is compatible with the bounds of z-variable in Ω_2, since for $r > 0$, it is $z \equiv r\cos\theta > 0$.

As for the conversion from the internal spherical to the cylindrical eigenfunctions to recover expansion (78), we rewrite $\lambda_n^m = r_n^m/\rho_L$ for $n \in \mathbb{N}$ and $m \in \mathbb{N}_+^*$, we weight both sides of (78) with $e^{-\lambda_n^m r}$ for $n \in \mathbb{N}$ and $m \in \mathbb{N}_+^*$, and we integrate with respect to the radial distance r to obtain

$$\int_0^{+\infty} J_n\left(\lambda_n^m r\sqrt{1-\zeta^2}\right)e^{-\lambda_n^m r(1-\zeta)}\mathrm{d}r = \sum_{n'=0}^{+\infty}\left[B_{n'/n}^{n/m}e^{\lambda_n^m z_0}\right]P_{n'}^{n}(\zeta)\int_0^{+\infty} r^{n'}e^{-\lambda_n^m r}\mathrm{d}r \text{ for } \mathbf{r}\in\Omega_2 \tag{84}$$

with $n \in \mathbb{N}$ and $m \in \mathbb{N}_+^*$, where, again, we have used the conversion relations $\rho = r\sqrt{1-\zeta^2}$ and $z = r\zeta$ to the left-hand side of relationship (84). The integral on the right-hand side of (84) bears standard treatment as follows:

$$\int_0^{+\infty} r^{n'}e^{-\lambda_n^m r}\mathrm{d}r = (-1)^{n'}\frac{d^{n'}}{d\left(\lambda_n^m\right)^{n'}}\int_0^{+\infty} e^{-\lambda_n^m r}\mathrm{d}r = (-1)^{n'}\frac{d^{n'}}{d\left(\lambda_n^m\right)^{n'}}\left(\frac{1}{\lambda_n^m}\right) = \frac{n'!}{\left(\lambda_n^m\right)^{n'+1}} \tag{85}$$

for $n \in \mathbb{N}$ and $m \in \mathbb{N}_+^*$, while $n' \geq 0$. The calculation of the first integral is more tedious and its calculation is based on the identity

$$\int_0^{+\infty} e^{-\alpha x}J_p(\beta x)\,\mathrm{d}x = \frac{\beta^{-p}\left(\sqrt{\alpha^2+\beta^2}-\alpha\right)^p}{\sqrt{\alpha^2+\beta^2}} \text{ for } \mathrm{Re}\left[p\right] > -1 \text{ and } \mathrm{Re}\left[\alpha \pm i\beta\right] > 0. \tag{86}$$

Setting $\alpha \to \lambda_n^m(1-\zeta)$ and $\beta \to \lambda_n^m\sqrt{1-\zeta^2}$, replacing $\zeta = \cos\theta$, fixing properly the index $p \to n$, changing the integration variable $x \to r$, and performing some algebraic calculations, and some simplifications of the trigonometric functions, then (86) converts to

$$\begin{aligned}\int_0^{+\infty} e^{-\lambda_n^m r(1-\zeta)}J_n\left(\lambda_n^m r\sqrt{1-\zeta^2}\right)\mathrm{d}r &= \frac{1}{2\lambda_n^m\sin(\theta/2)}\left[\frac{2\sin(\theta/2)-2\sin^2(\theta/2)}{\sin\theta}\right]^n \\ &= \frac{1}{2\lambda_n^m\sin(\theta/2)}\left[\frac{1-\sin(\theta/2)}{\cos(\theta/2)}\right]^n \text{ for } 0<\theta<\pi\end{aligned} \tag{87}$$

with $n \in \mathbb{N}$ and $m \in \mathbb{N}_+^*$, while the restrictions hold true, since obviously $\mathrm{Re}[n] \equiv n > -1$ and $\mathrm{Re}\left[\lambda_n^m\left(1-\zeta \pm i\sqrt{1-\zeta^2}\right)\right] \equiv \lambda_n^m(1-\zeta) > 0$. Putting all the analytical tools together, we substitute (85) and (87) into (84) for $\zeta = \cos\theta$, yielding

$$\sum_{n'=0}^{+\infty}\frac{n'!}{\left(\lambda_n^m\right)^{n'+1}}\left[B_{n'/n}^{n/m}e^{\lambda_n^m z_0}\right]P_{n'}^{n}(\cos\theta) = \frac{1}{2\lambda_n^m\sin(\theta/2)}\left[\frac{1-\sin(\theta/2)}{\cos(\theta/2)}\right]^n \text{ for } \mathbf{r}\in\Omega_2 \tag{88}$$

with $n \in \mathbb{N}$ and $m \in \mathbb{N}_+^*$, from which by projection of both sides on the elements of the associated Legendre functions and using the orthogonality relation

$$\int_0^\pi P_{n'}^n(\cos\theta) P_{\overline{n}}^n(\cos\theta) \sin\theta \mathrm{d}\theta = \frac{2}{2n'+1} \frac{(n'+n)!}{(n'-n)!} \delta_{n'\overline{n}} \text{ for } n, n' \in \mathbb{N}, \tag{89}$$

we get

$$B_{n'/n}^{n/m} = \frac{2n'+1}{4} \frac{(n'-n)!}{(n'+n)!} \frac{\left(\lambda_n^m\right)^{n'}}{n'!} e^{-\lambda_n^m z_0} \int_0^\pi \frac{\sin\theta P_{n'}^n(\cos\theta)}{\sin(\theta/2)} \left[\frac{1-\sin(\theta/2)}{\cos(\theta/2)}\right]^n \mathrm{d}\theta, \tag{90}$$

or, since $\sin\theta = 2\sin(\theta/2)\cos(\theta/2)$,

$$B_{n'/n}^{n/m} = \frac{2n'+1}{2} \frac{(n'-n)!}{(n'+n)!} \frac{\left(\lambda_n^m\right)^{n'}}{n'!} e^{-\lambda_n^m z_0} \int_0^\pi \frac{[1-\sin(\theta/2)]^n}{[\cos(\theta/2)]^{n-1}} P_{n'}^n(\cos\theta)\, \mathrm{d}\theta, \tag{91}$$

where $n, n' \in \mathbb{N}$, and $m \in \mathbb{N}_+^*$. Since $\lambda_n^m = r_n^m/\rho_L$ for $n \in \mathbb{N}$ and $m \in \mathbb{N}_+^*$, relationship (91) can be written in the compact form

$$B_{n'/n}^{n/m} = \frac{2n'+1}{2n'!} \frac{(n'-n)!}{(n'+n)!} \left(\frac{r_n^m}{\rho_L}\right)^{n'} e^{-\frac{r_n^m}{\rho_L} z_0} I_{n'}^n, \text{where } I_{n'}^n = \int_0^\pi \frac{[1-\sin(\theta/2)]^n}{[\cos(\theta/2)]^{n-1}} P_{n'}^n(\cos\theta)\, \mathrm{d}\theta, \tag{92}$$

which is the sought relation that coincides with the result of (71) for the surviving constants if $m' = n$ with $n, n' \in \mathbb{N}$ and $m \in \mathbb{N}_+^*$. The integral $I_{n'}^n$ depends only upon the indices n and n' but has to be evaluated numerically for each pair. Notice, however, that the integrand is a well-behaved function inside the integration interval, so the numerical integration is not to pose any particular problems. Finally, within the integral of (92), we must pay attention to the fact that $P_{n'}^n(\cos\theta) \equiv 0$ when $n > n'$, while again, here, integration over $\theta \in (0, \pi)$ in (92) reflects the positive sign of $\cos(\theta/2)$ as expected.

For the numerical validation of the conversion relations (77) and (78), by invoking the relative derived expressions for the coefficients (83) and (92), respectively, we compare for each case the modes, evaluated both directly and via (77) and (78) for a set of characteristic values of the involved parameters, and we compare the two results. The comparison for the spherical to cylindrical conversion is shown in Figure 2, whereas the corresponding results for the second conversion from cylindrical to spherical modes is presented in Figure 3.

There exist numerous of comparisons similar to those demonstrated within the aforementioned diagrams for different characteristic parameters; however, we have chosen to expose selectively some representative situations, which are sufficient for the validation. Observing the behavior of the spherical (see Figure 2) and the cylindrical (see Figure 3) eigenfunctions is excellent, and the obtained results coincide with the exact computation of these functions.

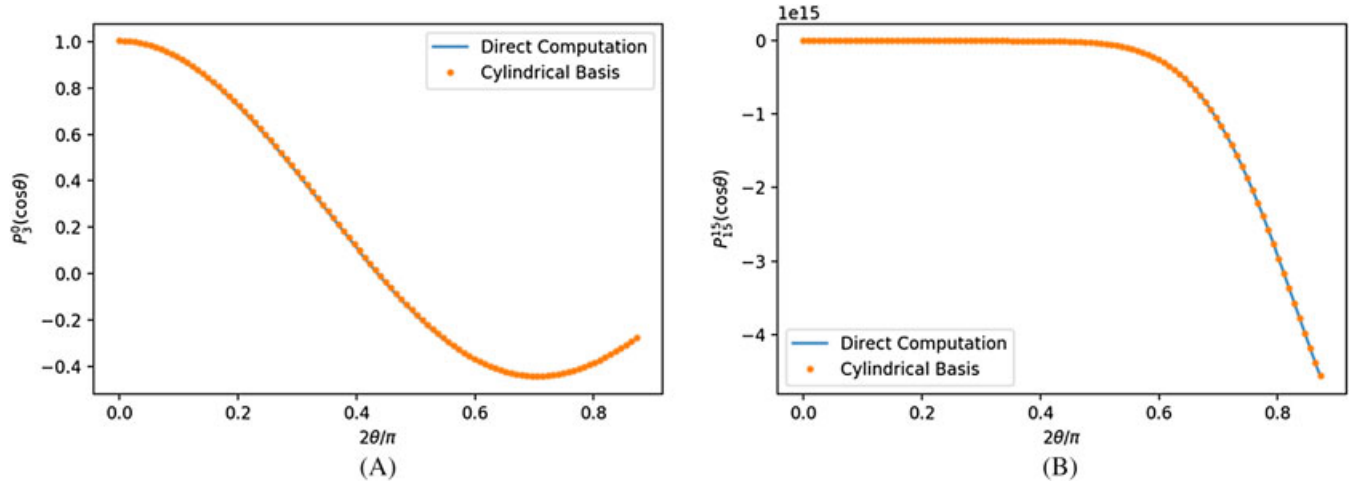

FIGURE 2 Spherical functions $P_{n'}^{m'}(\zeta) \equiv P_{n'}^{m'}(\cos\theta)$, evaluated in the interval $\theta \in [0, \pi/2]$ for different values (A) $n' = 3/m' = 0$ and (B) $n' = 15/m' = 15$, as for the order and the degree, respectively [Colour figure can be viewed at wileyonlinelibrary.com]

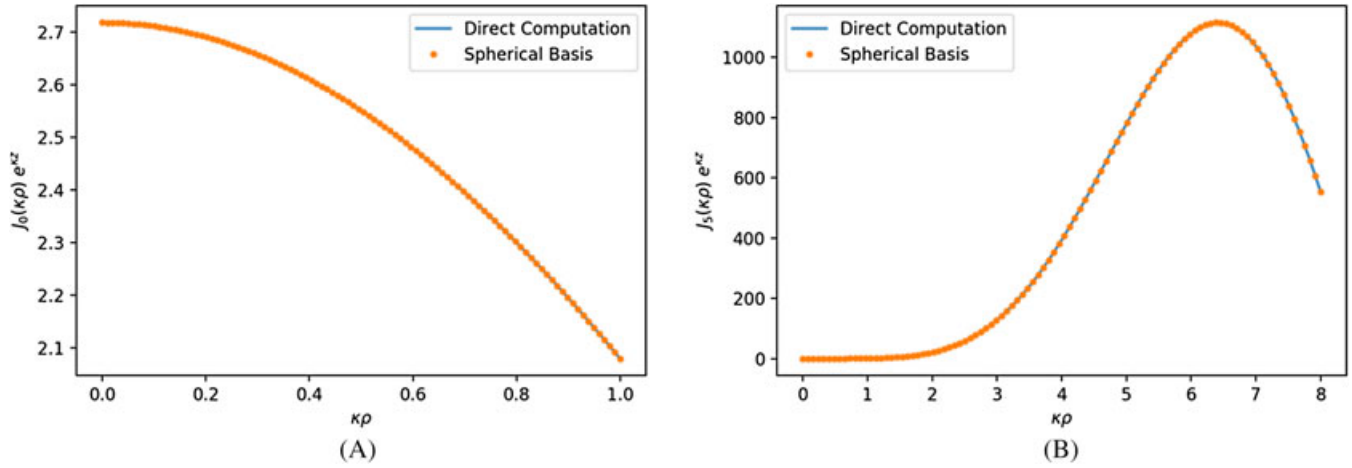

FIGURE 3 Cylindrical functions $J_n\left(r_n^m \rho/\rho_L\right) e^{\left(r_n^m/\rho_L\right)z} \equiv J_n(\kappa\rho)\, e^{\kappa z}$, evaluated at $z = 0.005$ mm and in the interval for $\rho \in [0, 0.1]$ mm when (A) $n = 0/\kappa = 10\ \text{mm}^{-1}$ and (B) $n = 5/\kappa = 80\ \text{mm}^{-1}$, as for the order and the constant of separation of variables, respectively [Colour figure can be viewed at wileyonlinelibrary.com]

5 - NUMERICAL IMPLEMENTATION FOR THE SPHERICAL INCLUSION

The aforementioned perfect validation of the derived expressions by comparison for each case of the modes, evaluated both directly and via the conversion relations for a set of characteristic values of the parameters, offers the perfect environment for the implementation stage to get involved thereafter. In view of this aspect, the corresponding numerical simulations are performed by the ACDC module of COMSOL Multiphysics software, which is based on a 3-D finite element method.

The displayed model has been applied to the considered circumstance depicted in Figure 1, where we consider a spherical inclusion and the ferromagnetic half-space of relative permeability $\mu_r = 100$ with respect to the air. Aiming to effectively mimic the introduced geometrical area and extend it far enough with respect to the observation domain, we truncate the magnetic activity zone by a cube of 50 mm each side. Hence, the limiting behavior of the theoretical analysis is consistent in the z-direction, while the cylindrical external boundary is set at $\rho_L = 50.0$ mm as a fair approximation to the perfect magnetic boundary condition. Besides, larger truncation radii have an almost negligible impact to the accuracy of the results, and simultaneously, computational consuming time is kept within logical bounds. By definition of the common center of the cylindrical and spherical coordinate systems, we presume a sphere of radius $r_s = 4.0$ mm, whose center coincides with the $(0, 0, 0)$ of the introduced geometry, being located 4.2 mm beneath the interface, ie, $z_0 = 4.2$ mm. On the other hand, the source field has an inner and outer radius of $r_{\text{in}} = 2.0$ mm and $r_{\text{out}} = 4.0$ mm, respectively; its length is $2d = 2.0$ mm and it is wound with 200 wire turns. The air-cored coil is moved at a fixed lift-off equal to 0.2 mm from the half-space interface, ie, $z_c - z_0 - d = 0.2$ mm, resulting to $z_c = 5.4$ mm, while the forthcoming results are taken for three different and randomly chosen displacements of the coil with respect to the z-axis of symmetry, ie, for $\rho_c = 0.0$ mm (Figure 4), $\rho_c = 1.0$ mm (Figure 5), and $\rho_c = 2.0$ mm (Figure 6).

On the other hand, the measurable field in cylindrical geometry is concerned with the radial B_ρ[=]mT and the axial B_z[=]mT components of the magnetostatic vector

$$\mathbf{B}(\mathbf{r}) = B_\rho(\rho, z)\, \hat{\boldsymbol{\rho}} + B_z(\rho, z)\, \hat{\mathbf{z}} \text{ for every } \mathbf{r} \equiv (\rho, \varphi, z) \in \Omega \tag{93}$$

with respect to the final formulae (49) to (51) for a spherical inclusion and accordingly to each subset domain of interest Ω_1, Ω_2, and Ω_v. Otherwise, magnetic induction $\mathbf{B}$ is a rotational symmetric field as a fair approximation of the modeling configuration, meaning that it is independent of the azimuthal angle $\varphi \in [0, 2\pi)$, ie, $\partial\mathbf{B}/\partial\varphi = \mathbf{0}$, and that its vector lives on a meridian plane, ie, $\hat{\boldsymbol{\varphi}} \cdot \mathbf{B} = 0$. Therein, field (93) is numerically implemented upon an observation line of constant z, parallel to the plane separating the half-space ferromagnetic material and the open air, situated at a constant depth of 4.9 mm from the interface, which stands for the observation region that ranges along the x-axis and it is providing measurements at $x \in [-30\ \text{mm}, 30\ \text{mm}]$, the two tips of this interval being taken at $\varphi = \pi$ and $\varphi = 0$, respectively, for $\rho = 30$ mm by virtue of $x = \rho\cos\varphi$ in cylindrical coordinates. Obviously, since the direction of this line coincides with the ρ-direction shown

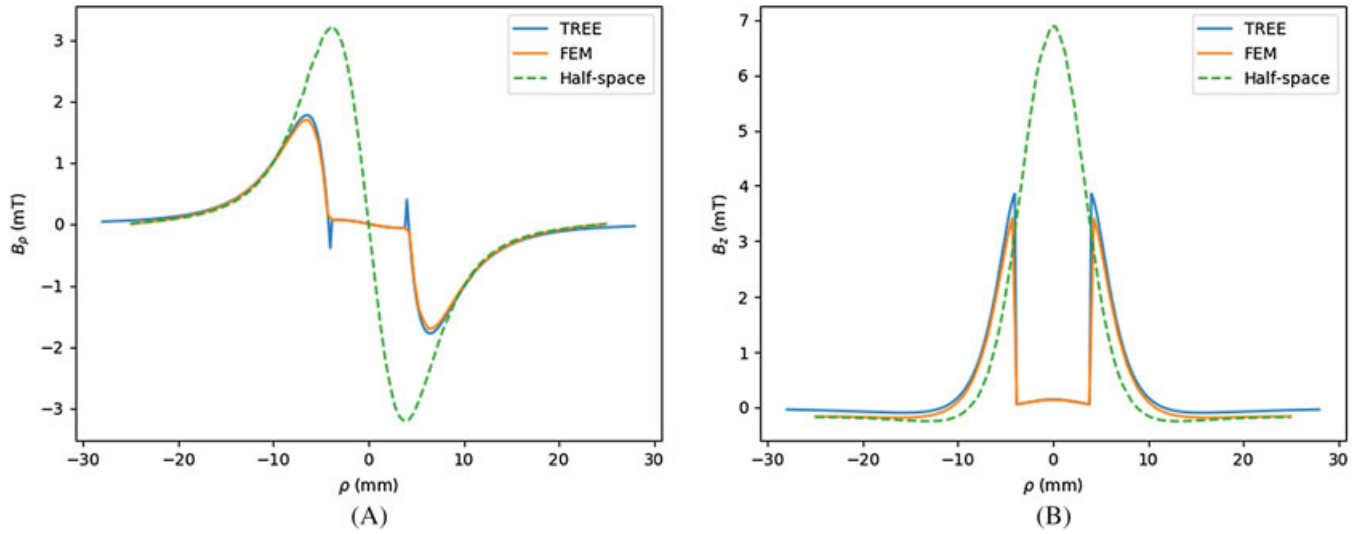

FIGURE 4 Semianalytical (blue line) versus finite element method (FEM) simulation (orange line) results of the magnetostatic components (A) B_ρ[=]mT and (B) B_z[=]mT for a spherical inclusion of prescribed radius 4.0 mm and location 4.2 mm beneath the interface, the green dashed line referring to the case of no inclusion. The air-cored coil source is moved at a fixed lift-off equal to 0.2 mm and its displacement is 0.0 mm with respect to the z-axis of symmetry [Colour figure can be viewed at wileyonlinelibrary.com]

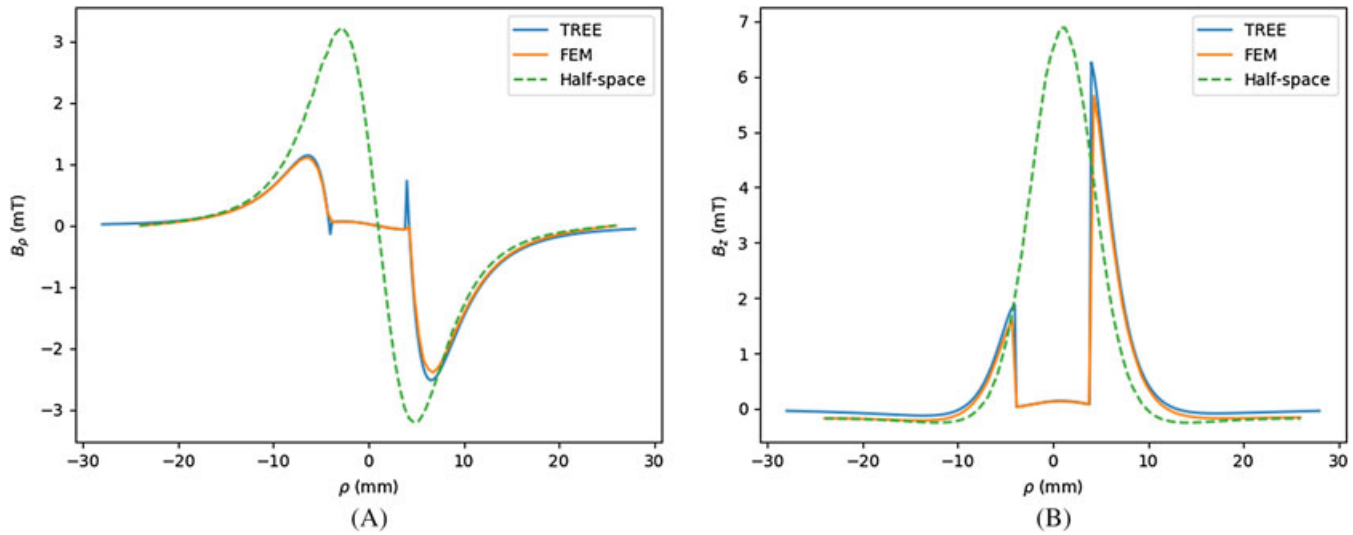

FIGURE 5 Semianalytical (blue line) versus finite element method (FEM) simulation (orange line) results of the magnetostatic components (A) B_ρ[=]mT and (B) B_z[=]mT for a spherical inclusion of prescribed radius 4.0 mm and location 4.2 mm beneath the interface, the green dashed line referring to the case of no inclusion. The air-cored coil source is moved at a fixed lift-off equal to 0.2 mm and its displacement is 1.0 mm with respect to the z-axis of symmetry [Colour figure can be viewed at wileyonlinelibrary.com]

in Figure 1, the x-variable matches the cylindrical component; hence, for reasons of numerical convenience within (93), we mutually expand the ρ-dependence to negative values as well. For a better qualitative understanding of the results, we provide simultaneously the corresponding response of the magnetostatic field in the absence of the spherical inclusion and we embody this characteristic situation in the same diagram for each case to demonstrate the direct effect of the inclusion to the field behavior. As depicted in Figure 4, setting the source's center on the z-axis, just above the spherical inclusion, we attain a symmetric situation, readily reflected upon the behavior of the field, which is not the case of a different displacement of the source, as shown in Figures 5 and 6, where we observe that as we move far away from the axis of symmetry, the field's response deviates from the initial condition, which is logic and agrees with reality.

The respective finite element method calculation time instead is estimated to 1.5 minutes per scan point, both times being measured using a standard PC workstation. It should be pointed out that the computational effort for the semianalytical solution is independent to the number of scan points because the system matrix is independent of the coil position,

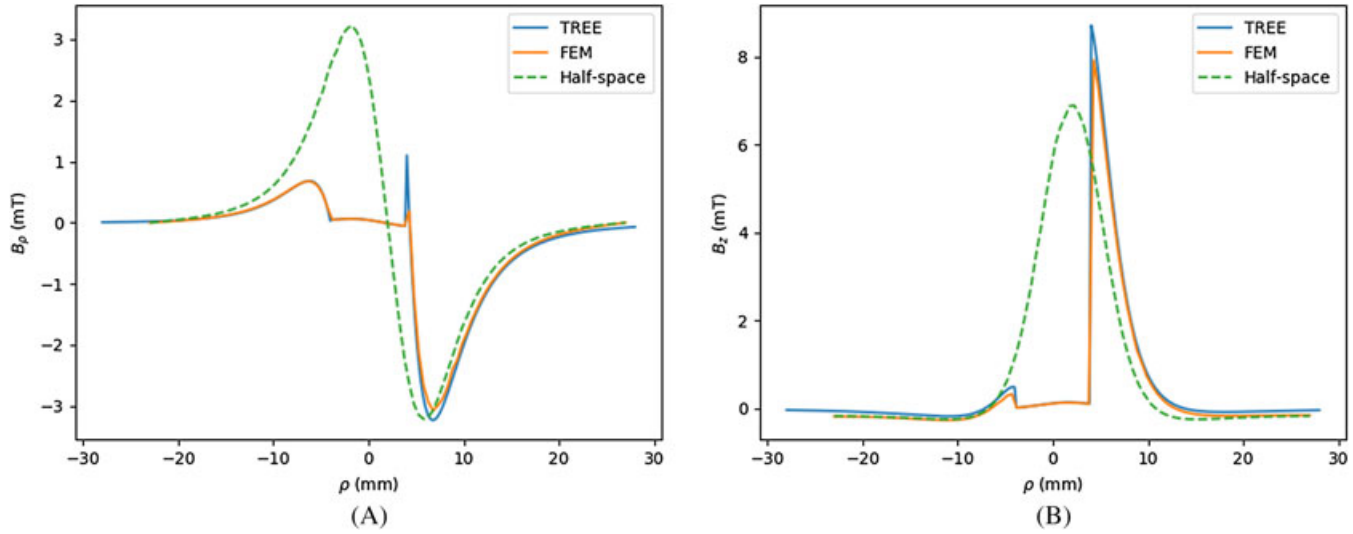

FIGURE 6 Semianalytical (blue line) versus finite element method simulation (orange line) results of the magnetostatic components (A) B_ρ[=]mT and (B) B_z[=]mT for a spherical inclusion of prescribed radius 4.0 mm and location 4.2 mm beneath the interface, the green dashed line referring to the case of no inclusion. The air-cored coil source is moved at a fixed lift-off equal to 0.2 mm and its displacement is 2.0 mm with respect to the z-axis of symmetry [Colour figure can be viewed at wileyonlinelibrary.com]

the latter affecting only the right-hand side vector of the linear system. Therefore, using LU variants for the system inversion, the additional computational cost is merely due to the backwards substitution calculations, which is a well-reported advantage of semianalytical solutions. The reason for the very small calculation times lies also with the rapid convergence of the solution series, which allowed us to consider few modes. This is not surprising, since the cylindrical and spherical potential functions bases used for the solution expansion are partial solutions of the given geometry, and thus, they are already very close to the final solution.

Recapitulating, we should emphasize the fact that the efficiency of the presented general model provides a powerful tool in producing analytical or semianalytical results. This statement is valid not only for magnetostatic problems as in our case but also could serve other engineering applications near this field, helping in the achievement of usefully analytical modes as a reference point for more brute-force numerical codes.

6 - CONCLUSIONS AND DISCUSSION

A semianalytical method to the magnetostatic scattering problem for an air inclusion in a conducting ferromagnetic half-space, excited by an air-cored coil source, has been developed. The general technique for the identification of an arbitrarily shaped hollow inclusion is presented based on rigorous, yet versatile mathematical tools. The continuity coupling between the two interfaces is taken into account via transmission conditions, while the limiting behavior of the fields is readily secured. The boundary approximation of a vanishing field at sufficiently long distance from the source creates an error of minor significance, since it can be made arbitrarily small just by fixing the truncation distance. Our generalized model is demonstrated by an application, where the inclusion is considered spherical and the solution provides adequate results, almost perfectly fitting numerical simulation. Hence, this comparison validates the efficiency of the proposed formulation.

Such analytical solutions and formulae in closed forms are always in the front line of scientific research and have important advantages compared with the pure numerical methods. Indeed, the validity of numerical solutions can be verified by analytical or semianalytical techniques. On the other hand, bearing in mind that very important physical laws can be derived from analytical methods, we can understand the necessity of a stable and secure mathematical basis for starting a numerical procedure. Therefore, even nowadays, there is always room for such kind of methods that coexist with pure numerical codes and aim to the solution of boundary value problems in physical applications of importance.

Mathematical and computational work is currently in progress and involves research into several directions, such as the involvement of more intricate geometries for the void inclusion or the creation of time-consuming brute-force inversion algorithms, taking profit from the simple framework proposed. For example, the general case of a 3-D ellipsoidal air

inclusion is far more elaborating than the spherical and the spheroidal one due to two (among others) main reasons. First, the involved potentials in ellipsoidal geometry are written in terms of elliptic integrals, which can be only manipulated numerically, and second, only few ellipsoidal harmonics render a fully analytical conformation; therefore, the task of writing cylindrical to ellipsoidal eigenfunctions and vice versa becomes very difficult.

ORCID

Panayiotis Vafeas http://orcid.org/0000-0002-0896-4168

REFERENCES

1. Stratton JA. *Electromagnetic Theory*. New York, NY: McGraw-Hill; 1941.
2. Dassios G, Kleinman RE. *Low Frequency Scattering*. Oxford, UK: Oxford University Press; 2000.
3. Ammari H, Garnier J, Jing W, et al. *Mathematical and Statistical Methods for Multistatic Imaging*. Cham, Switzerland: Springer International Publishing; 2013. *Lecture Notes in Mathematics*; vol. 2098.
4. Ammari H, Kang H. *Polarization and Moment Tensors With Applications to Inverse Problems and Effective Medium Theory*. New York, NY: Springer Science+Business Media; 2007. *Applied Mathematical Sciences Series*; vol. 162.
5. Ammari H, Dassios G, Kang H, Lim M. Estimates for the electric field in the presence of adjacent perfectly conducting spheres. *Quart Appl Math*. 2007;65(2):339-355.
6. Ammari H, Kang H, Lee H, Lim M, Zribi H. Decomposition theorems and fine estimates for electrical fields in the presence of closely located circular inclusions. *J Differ Equ*. 2009;247(11):2897-2912.
7. Björkberg J, Kristensson G. Three-dimensional subterranean target identification by use of optimization techniques. *Prog Electromagn Res*. 1997;15:141-164.
8. Yu T, Carin L. Analysis of the electromagnetic inductive response of a void in a conducting-soil background. *IEEE Trans Geosci Remote Sens*. 2000;38(3):1320-1327.
9. Huang H, Won IJ. Detecting metal objects in magnetic environments using a broadband electromagnetic method. *Geophysics*. 2003;68(6):1877-1887.
10. Chen X, O'Neill K, Barrowes BE, Grzegorczyk TM, Kong JA. Application of a spheroidal-mode approach and a differential evolution algorithm for inversion of magneto-quasistatic data in UXO discrimination. *Inverse Probl*. 2004;20(6):527-540.
11. Cui TJ, Aydiner AA, Chew WC, Wright DL, Smith DV. Three-dimensional imaging for buried objects in a very lossy earth by inversion of VETEM data. *IEEE Trans Geosci Remote Sens*. 2003;41(10):2197-2210.
12. Athanasiadis C, Martin PA, Stratis IG. Electromagnetic scattering by a homogeneous chiral obstacle: boundary integral equations and low-chirality approximations. *SIAM J Appl Math*. 1999;59(5):1745-1762.
13. Athanasiadis C, Martin PA, Stratis IG. Electromagnetic scattering by a homogeneous chiral obstacle: scattering relations and the far-field operator. *Math Methods Appl Sci*. 1999;22(14):1175-1188.
14. Athanasiadis C, Costakis G, Stratis IG. Electromagnetic scattering by a homogeneous chiral obstacle in a chiral environment. *IMA J Appl Math*. 2000;64(3):245-258.
15. Athanasiadis C, Costakis G, Stratis IG. Electromagnetic scattering by a perfectly conducting obstacle in a homogeneous chiral environment: solvability and low-frequency theory. *Math Meth Appl Sci*. 2002;25(11):927-944.
16. Vafeas P, Perrusson G, Lesselier D. Low-frequency solution for a perfectly conducting sphere in a conductive medium with dipolar excitation. *Prog Electromagn Res*. 2004;49:87-111.
17. Vafeas P, Perrusson G, Lesselier D. Low-frequency scattering from perfectly conducting spheroidal bodies in a conductive medium with magnetic dipole excitation. *Int J Eng Sci*. 2009;47(3):372-390.
18. Perrusson G, Vafeas P, Lesselier D. Low-frequency dipolar excitation of a perfect ellipsoidal conductor. *Quart Appl Math*. 2010;68(3):513-536.
19. Vafeas P, Papadopoulos PK, Lesselier D. Electromagnetic low-frequency dipolar excitation of two metal spheres in a conductive medium. *J Appl Math*. 2012;2012:1-37. Article ID 628261.
20. Perrusson G, Vafeas P, Chatjigeorgiou IK, Lesselier D. Low-frequency on-site identification of a highly conductive body buried in Earth from a model ellipsoid. *IMA J Appl Math*. 2015;80(4):963-980.
21. Vafeas P, Lesselier D, Kariotou F. Estimates for the low-frequency electromagnetic fields scattered by two adjacent metal spheres in a lossless medium. *Math Meth Appl Sci*. 2015;38(17):4210-4237.
22. Vafeas P, Papadopoulos PK, Ding P-P, Lesselier D. Mathematical and numerical analysis of low-frequency scattering from a PEC ring torus in a conductive medium. *App Math Model*. 2016;40(13-14):6477-6500.
23. Vafeas P. Low-frequency electromagnetic scattering by a metal torus in a lossless medium with magnetic dipolar illumination. *Math Meth Appl Sci*. 2016;39(14):4268-4292.
24. Mie G. Beiträge zur optik trüber medien, speziell kolloidaler metallösungen. *Ann Phys*. 1908;330(3):377-445.
25. Bobbert PA, Vlieger J. Light scattering by a sphere on a substrate. *Phys A Stat Mech Appl*. 1986;137(1-2):209-242.
26. Videen G. Light scattering from a sphere on or near a surface. *J Opt Soc Am A*. 1991;8(3):483-489.

27. Theodoulidis TP, Kantartzis NV, Tsiboukis TD, Kriezis EE. Analytical and numerical solution of the eddy-current problem in spherical coordinates based on the second-order vector potential formulation. *IEEE Trans Magn*. 1997;33(4):2461-2472.
28. Skarlatos A, Theodoulidis T. Semi-analytical calculation of the low-frequency electromagnetic scattering from a near-surface spherical inclusion in a conducting half-space. *Proc R Soc A*. 2014;470(2170):20140269.
29. Theodoulidis TP, Bowler JR. Eddy current coil interaction with a right-angled conductive wedge. *Proc R Soc A*. 2005;461(2062):3123-3139.
30. Theodoulidis TP, Bowler JR. Impedance of an induction coil at the opening of a borehole in a conductor. *J Appl Phys*. 2008;103(2):024905.
31. Skarlatos A, Theodoulidis T. Solution to the eddy-current induction problem in a conducting half-space with a vertical cylindrical borehole. *Proc R Soc A*. 2012;468(2142):1758-1777.
32. Skarlatos A, Theodoulidis T. Analytical treatment of eddy-current induction in a conducting half-space with a cylindrical hole parallel to the surface. *IEEE Trans Magn*. 2011;47(11):4592-4599.
33. Morse PM, Feshbach H. *Methods of Theoretical Physics*. Vol. 1. New York, NY: McGraw-Hill; 1953.
34. Hobson EW. *The Theory of Spherical and Ellipsoidal Harmonics*. New York, NY: Chelsea Publishing Company; 1965.
35. Abramowitz M, Stegun IA. *Handbook of Mathematical Functions With Formulas, Graphs, and Mathematical Tables*. Mineola, NY: Dover Publications; 1972.
36. Gradshteyn I, Ryzhik IM. In: Jeffrey A, Zwillinger D, eds. *Table of Integrals, Series and Products*. 7th ed. Burlington, MA: Academic Press; 2007.